Metabolic Network Failures in Alzheimer's Disease

- A Biochemical Roadmap

Jon B. Toledo[a,b*], Matthias Arnold[c], Gabi Kastenmüller[c,d], Rui Chang[e] , Rebecca A Baillie[f], Xianlin Han[g], Madhav Thambisetty[h], Jessica D. Tenenbaum[i], Karsten Suhre[c,j], J Will Thompson[k], Lisa St. John-Williams[k], Siamak MahmoudianDehkordi[l], Daniel M. Rotroff[d], John R. Jack[l], Alison Motsinger-Reif[d], Shannon L. Risacher[m], Colette Blach[i], Joseph E. Lucas[n], Tyler Massaro[n], Gregory Louie[o], Hongjie Zhu[o], Guido Dallmann[p], Kristaps Klavins[p]; Therese Koal[p], Sungeun Kim[m], Kwangsik Nho[m], Li Shen[m], Ramon Casanova[h], Sudhir Varma[h], Cristina Legido-Quigley[q], M. Arthur Moseley[k], Kuixi Zhu[e], Marc Henrion[e], Sven J van der Lee[r], Amy C. Harms[s], Ayse Demirkan[r], Thomas Hankemeier[r,s], Cornelia M. van Duijn[r,s], John Q. Trojanowski[a], Leslie M. Shaw[a], Andrew J. Saykin[m], Michael W. Weiner[t], P. Murali Doraiswamy[o], Rima Kaddurah-Daouk[o*] for the Alzheimer's Disease Neuroimaging Initiative and the Alzheimer Disease Metabolomics Consortium**

[a]Department of Pathology & Laboratory Medicine, University of Pennsylvania, Philadelphia, PA, USA; [b]Department of Neurology, Houston Methodist Hospital, Houston, TX, USA; [c]Institute of Bioinformatics and Systems Biology, Helmholtz Zentrum München, German Research Center for Environmental Health, Neuherberg, Germany; [d]German Center for Diabetes Research (DZD), Neuherberg, Germany; [e]Department of Genetics and Genomic Science, Icahn School of Medicine at Mount Sinai, New York, NY, USA; [f]Rosa & Co LLC, San Carlos, CA, USA; [g]Sanford Burnham Prebys Medical Discovery Institute, Orlando, FL, USA; [h]Clinical and Translational Neuroscience Unit, Laboratory of Behavioral Neuroscience, National Institute on Aging, National Institutes of Health, Baltimore, MD, USA; [i]Duke Molecular Physiology Institute, Duke University, Durham, NC, USA; Department of Biostatistics and Bioinformatics, Duke University, Durham, NC, USA; [j]Department of Physiology and Biophysics, Weill Cornell Medical College, Qatar, Doha, Qatar; [k]Duke Proteomics and Metabolomics Shared Resource, Center for Genomic and Computational Biology; [l]Bioinformatics Research Center, Department of Statistics, North Carolina State University, Raleigh, NC, USA; [m]Department of Radiology and Imaging Sciences

**Data used in preparation of this article were obtained from the Alzheimer's Disease Neuroimaging Initiative (ADNI) database (adni.loni.usc.edu). As such, the investigators within the ADNI contributed to the design and implementation of ADNI and/or provided data but did not participate in analysis or writing of this report. A complete listing of ADNI investigators can be found at: http://adni.loni.usc.edu/wp-content/uploads/how_to_apply/ADNI_Acknowledgement_List.pdf.

and the Indiana Alzheimer Disease Center, Indiana University School of Medicine, Indianapolis, IN, USA; [n]Institute for Genome Sciences and Policy, Duke University, Durham, NC, USA; [o]Department of Psychiatry and Behavioral Sciences, and the Duke Institute for Brain Sciences, Duke University, Durham, NC, USA; [p]BIOCRATES Life Sciences AG, Innsbruck, Austria; [q]IPS, Faculty of Live Sciences and Medicine, King's College London, London; [r]Department of Epidemiology, ErasmusMC, Postbus 2040, 3000 CA Rotterdam, The Netherlands; [s]Analytical Biosciences, Leiden Academic Centre for Drug Research, Leiden University, Leiden, Netherlands; [t]Center for Imaging of Neurodegenerative Diseases, Department of Radiology, San Francisco VA Medical Center/University of California San Francisco, San Francisco, CA.

Address correspondence to:

Rima Kaddurah-Daouk PhD, Department of Psychiatry and Behavioral Sciences, Department of Medicine, Duke Institute for Brain Sciences Duke University, Durham, NC, USA Tel- 919-684-2611

Email: kaddu001@mc.duke.edu

Jon Toledo MD, PhD, Department of Neurology, Houston Methodist Hospital, Houston, TX, USA

Email: jbtoledoatucha@houstonmethodist.org

Abbreviations:

α-AAA: α-Aminoadipic acid; AD: Alzheimer disease; ADAS-Cog13: Alzheimer's Disease Assessment Scale-Cognition; ADMC: Alzheimer Disease Metabolomics Consortium; *APOE*: apolipoprotein E; BCAA: branched-chain amino acid; BIC: Bayesian information criteria; C0: free carnitine; CN: Cognitively normal; CSF: Cerebrospinal fluid; Cx:y: acylcarnitines; Cx:y-DC: dicarboxylacylcarnitines; Cx:y-OH: hydroxylacylcarnitines, ERF: Erasmus Rucphen Family; FIA: Flow injection analysis; GGM: Gaussian graphical model; lysoPC: lyso-glycero-phosphatidylcholines (a=acyl); MCI: Mild cognitive impairment; IMAS: Indiana Memory and Aging Study; LOD: Limit of detection; MMSE: Mini mental state examination; NIA: National Institute on Aging; Path. $A\beta_{1-42}$: Pathological $A\beta_{1-42}$; PC: glycero-phosphatidylcholines (aa=diacyl, ae=acyl-alkyl); PC ae: Ether-containing PC; PET: Positron emission

tomography; PiB: Pittsburgh Compound B; PS: Presenilin; QC: Quality control; SDMA: Symmetric dimethylarginine; SM: Sphingomyelin; SM (OH) x:y: N-hydroxylacyloylsphingosyl-phosphocholine; SPARE-AD: Spatial Pattern of Abnormalities for Recognition of Early AD; SSRI: selective serotonin re-uptake inhibitors; T4-OH-Pro: trans-4-Hydroxyproline; t-tau: total tau; UPLC: ultra-performance liquid chromatography.

Highlights

1. Metabolomics analysis guided by CSF biomarker and imaging data provide novel mechanistic insights about Alzheimer's disease (AD), information that can guide novel approaches for drug discovery.

2. Early biochemical changes in AD are noted that precede cognitive changes and that inform about biochemical dysfunctions related to Aβ and tau pathology.

3. Peripheral metabolic profile of patients informs about trajectory of disease progression, disease subtypes and can lead to development of valuable biomarkers for accelerating clinical trials.

4. Metabolic network failures in AD provide a systems approach for the study of the disease in line with recommendations of AD Summits of 2012 and 2015.

ABSTRACT

INTRODUCTION:

The Alzheimer's Disease Research Summits of 2012 and 2015 incorporated experts from academia, industry and non-profit organizations to develop new research directions to transform our understanding of Alzheimer's disease (AD) and propel the development of critically needed therapies. In response to their recommendations, big data at multiple levels are being generated and integrated to study network failures in disease. We used metabolomics as a global biochemical approach to identify peripheral metabolic changes in AD patients and correlate them to cerebrospinal fluid pathology markers, imaging features, and cognitive performance.

METHODS:

Fasting serum samples from the Alzheimer's Disease Neuroimaging Initiative (199 control, 356 mild cognitive impairment and 175 AD participants) were analyzed using the AbsoluteIDQ®-p180 kit. Performance was validated in blinded replicates, and values were medication adjusted.

RESULTS:

Multivariable adjusted analyses showed that sphingomyelins and ether-containing phosphatidylcholines were altered in preclinical biomarker-defined AD stages, whereas acylcarnitines and several amines, including the branched chain amino acid valine and α-aminoadipic acid, changed in symptomatic stages. Several of the analytes showed consistent associations in the Rotterdam, Erasmus Rucphen Family, and Indiana Memory and Aging Studies. Partial correlation networks constructed for $A\beta_{1-42}$, Tau, imaging and cognitive changes provided initial biochemical insights for disease-related processes. Co-expression networks interconnected key metabolic effectors of disease.

DISCUSSION:

Metabolomics identified key disease-related metabolic changes and disease-progression-related changes. Defining metabolic changes during AD disease trajectory and its relationship to clinical phenotypes provides a powerful roadmap for drug and biomarker discovery.

Keywords: metabolomics, metabonomics, pharmacometabolomics, pharmacometabonomics, biomarkers, serum, metabolism, systems biology, biochemical networks, precision medicine, Alzheimer's disease, dementia, branched chain amino acids, sphingomyelins, phospholipids, acylcarnitines.

1. INTRODUCTION

Alzheimer's disease (AD) is the most common cause of dementia. An anticipated 136 million people will be affected by dementia by 2050, presenting major global health and economic challenges. There are currently no treatments that modify AD, hence AD remains the largest unmet medical need within neurological disorders [1, 2].

Many biochemical processes are affected in AD, including amyloid precursor protein metabolism, phosphorylation of tau protein, oxidative stress, impaired energetics, mitochondrial dysfunction, inflammation, membrane lipid dysregulation and neurotransmitter pathway disruption [3, 4]. Impaired cerebral glucose uptake occurs decades prior to the onset of cognitive dysfunction in AD [5], and neurotoxicity associated with Aβ is thought to participate in impaired neuronal energetics including mitochondrial dysfunction and release of reactive oxygen species. Growing evidence supports the concept that insulin resistance can contribute to AD pathogenesis, and therefore, AD could be regarded as a metabolic disease mediated in part by brain insulin and insulin-like growth factor resistance [3]. Mapping the trajectory of biochemical changes in AD is therefore becoming a priority as filling knowledge gaps about disease mechanisms and their link to metabolic processes can lead to developing much-needed biomarkers and therapies [3]. How does peripheral metabolism, diet, gut microbiome, and exposome impact the metabolic heath of the brain, and thus cognitive function? Which pathways are affected by genes that have been implicated in AD, such as presenilin 1 (PSEN1) and PS2 or apolipoprotein E (APOE)? Biochemical information elucidating these questions is critical for developing drugs that target enzymes and transporters which regulate metabolism.

Metabolomics provides powerful tools for mapping global biochemical changes in disease and treatment [6-10]. In contrast to classical biochemical approaches that focus on single metabolites or reactions, metabolomics and lipidomics approaches simultaneously identify and quantify hundreds to thousands of

metabolites [11-19]. Measurement of large numbers of metabolites enables network analysis approaches and provides means to identify critical metabolic drivers in disease pathophysiology [20]. Initial small scale metabolomics studies in AD have highlighted metabolic alterations including ceramide-sphingomyelin pathways [10], PC [15, 21], PE plasmalogens [22, 23], amines [24], and mitochondrial defects [25] among others [13, 14]. Metabolic networks have linked central perturbations in norepinephrine and purines with elevated cerebrospinal fluid (CSF) tau, and changes in tryptophan and methionine to decreased Aβ levels [18]. More recently, the ARIC Neurocognitive Study identified PC aa C36:1 as being linked to lower risk of dementia; however, no metabolite from the panel measured added significantly to prediction of dementia beyond routine clinical variables [26]. A recent plasma-pathology correlative study found that plasma ceramides C16:0, C18:1, C20:0 and C24:1 and monohexosylceramides C18:1 and C24:1 were elevated in those with autopsy-confirmed AD pathology [27], but these metabolites did not differentiate AD from dementia with Lewy bodies. An autopsy study of frontal cortex metabolites from AD patients versus controls showed six central metabolic pathways were altered along with glycerophospholipid metabolism and aspartate metabolism. A metabolomics study in an AD mouse model (APPswe/PS1deltaE9 double transgenic) found abnormalities in polyamine metabolism, essential amino acids, BCAAs, and serotonin, as well as phospholipid and acylcarnitine homeostasis with brain changes preceding those in the blood [28]. While these studies highlight specific metabolic underpinnings of AD, not all metabolomics findings have been replicated. For example, a metabolomics study of two separate cohorts − the Baltimore Longitudinal Study of Aging, and the Age, Gene/Environment Susceptibility-Reykjavik Study – did not replicate an earlier finding [11, 12, 15].

Earlier metabolomics studies had major limitations, including not accounting for important confounds such as impact of medications use; small studies that lacked evaluation across datasets; limited ability to connect peripheral metabolic changes with central changes to define what might be related, and lack of attempts to connect metabolic changes within a pathway and network context. Network biology and 'network medicine' approaches have become important tools to dissect molecular mechanisms triggering

neurodegeneration [29].This approach accounts for the fact that complex diseases arise from alterations in multiple genes, proteins and metabolites, and a network may be described as an interaction map among the wide range of biological entities which contribute to disease. As many of the metabolites that are associated with AD are interconnected through metabolic pathways, co-factors, and common intermediates, changes to one metabolite can entail several others, as well as have downstream effects on other co-regulated pathways. A systems biology approach integrating metabolites and their interrelations (for instance quantified by partial correlations) in metabolic networks can provide important mechanistic insights about how biochemical reactions are dysregulated during different stages of disease. In contrast to looking at single dysregulated metabolite at a time, the visualization of changes in the metabolic network captures the totality of influences on interconnected biochemical reactions in far more informative ways and allows one to follow these changes over disease stages.

In this large study, we profiled baseline serum samples from the Alzheimer's Disease Neuroimaging Initiative -1 (ADNI-1) cohort where vast data exist on each patient including cognitive decline and imaging changes over many years, information on CSF markers, genetics and other omics data. We used CSF biomarkers to define early metabolic changes in cognitively normal participants who have CSF pathology, and to evaluate metabolic signatures that might be related to $A\beta_{1-42}$ and tau pathology. Using partial correlation networks, we defined progressive metabolic changes that accompany changes in CSF $A\beta_{1-42}$, CSF tau, brain structure and cognition [30], while co-expression networks were used to connect key metabolic changes implicated in disease. The relationship of metabolites with longitudinal cognitive and imaging changes helped us define metabolic signatures correlated with disease progression. Key associations were also present in multiple independent cohorts. We believe that the systems approach taken in our study to elucidate metabolic changes along different stages during the progression of AD will transform our understanding of disease mechanisms and lead to valuable peripheral biomarkers that can inform and accelerate clinical trials.

2. METHODS

2.1 Study Cohorts and Samples

A. ADNI-1 baseline samples

ADNI shipped 831 samples with unique identifiers belonging to 807 subjects. These initial identifiers were different from the ADNI subject identifiers. There were duplicate aliquots from the same CSF draw for 24 subjects to help us evaluate analytical performance. Only after the final raw data was submitted to ADNI, was the information obtained to link the samples identifier to the subject RID and identify the duplicates.

Data were obtained from the ADNI database in September 2015 (http://adni.loni.usc.edu). ADNI-1 was launched in 2004 by the National Institute on Aging (NIA), the National Institute of Biomedical Imaging and Bioengineering, the Food and Drug Administration, private pharmaceutical companies and non-profit organizations [31]. ADNI-1 patients underwent extensive clinical and cognitive testing, including the Alzheimer's Disease Assessment Scale-Cognition (ADAS-Cog13), which was used as a measure of general cognition in this analysis. AD dementia diagnosis was established based on the NINDS-ADRDA criteria for probable AD. Mild cognitive impairment (MCI) participants did not meet these AD criteria and had largely intact functional performance, meeting predetermined criteria for amnestic MCI [31]. Controls were cognitively normal (CN) (**Supplementary Table 1**). Additional details of participant selection criteria and protocol are available at http://www.adni-info.org and in the methods in the **Supplementary Materials**. The study was approved by institutional review boards of all participating institutions and written informed consent was obtained from all participants and/or authorized representatives prior to study commencement.

B. Rotterdam and Erasmus Rucphen Family (ERF) Cohorts

Participants from the Erasmus Rucphen Family (ERF) study (N=905) were metabolically profiled from fasting blood samples using the Biocrates AbsoluteIDQ p150 kit platform (**Supplementary Table 2**) [32], which measures a subset of metabolites from the P180 and excludes many of the amines. A previously described quality control (QC) protocol was applied [32]. Valine was measured in fasting blood samples using the brainshake® platform [33] in 2,752 participants from the Rotterdam large prospective cohort study [34]. Participants of the ERF study underwent a standardized cognitive test battery at the study center on the same day blood was drawn (**Supplementary Table 2**) [35]. Participants of the Rotterdam study underwent cognitive tests at the time of valine measurement and all participants were followed up for AD clinical diagnosis [36], as previously described in detail [37].

The general cognitive ability or '*g*-factor' was calculated using previously described methods in dementia-free participants with available cognitive tests in the ERF study (N=905) and Rotterdam Study (N=2480) [38]. In short, the *g*-factor is a general cognitive function phenotype created by principal component analysis of multiple cognitive tests. A higher *g*-factor is associated with a higher general cognitive function, in contrast to the cognitive measure used for analysis of the ADNI-1 cohort, the ADAS-Cog13.

C. The Indiana Memory and Aging Study (IMAS):

IMAS is an ongoing longitudinal study investigating multimodal neuroimaging, cognition, fluid biomarkers, and genetics in early prodromal stages of AD with follow-up visits every 18 months [39-42]. IMAS participants included CN participants, euthymic older adults with subjective cognitive decline in the absence of significant psychometric deficits, and patients with amnestic MCI or probable AD (**Supplementary Table 3**). Due to limited sample size compared to other cohorts, analyses were limited to assessment of [^{11}C] Pittsburgh Compound B (PiB) positron emission tomography (PET) amyloid status. Thirty four participants had PET scans to measure brain Aβ load; 30 participants underwent [^{11}C]PiB PET scans on a Siemens HR+ PET scanner and 4 participants underwent [^{18}F]Florbetapir PET

scans on a Siemens mCT. For the [^{11}C]PiB PET, participants underwent either a 90-minute dynamic scan starting at time of tracer injection or a 50-minute dynamic scan after a 40-minute uptake period after injection of approximately 10mCi of [^{11}C]PiB. The [^{18}F]Florbetapir PET scans were collected as a 30-minute dynamic scan after a 40-minute uptake period following an injection of approximately 10mCi of [^{18}F]Florbetapir. [^{11}C]PiB and [^{18}F]Florbetapir scans were motion-corrected and normalized to Montreal Neurologic Institute (MNI) space using parameters from a same timepoint structural MRI scan. For the [^{11}C]PiB PET images, a 40-90 minute standardized uptake value ratio (SUVR) image was created by averaging the appropriate frames and intensity normalizing to mean cerebellar grey matter uptake. For the [^{18}F]Florbetapir PET, a 40-70 minute SUVR image was created by averaging the appropriate frames and intensity normalizing to mean whole cerebellar uptake. Finally, amyloid positivity was defined as a mean [^{11}C]PiB PET SUVR of ≥ 1.37 or a mean [^{18}F]Florbetapir SUVR of ≥ 1.20 from a cortical grey matter region of interest (ROI). These cut-offs were determined by simultaneous processing of the ADNI [^{11}C]PiB and [^{18}F]Florbetapir PET images using the same pipeline and adjusting the locally-derived cut-offs to best match either the previously reported [^{11}C]PiB PET cut-off of mean cortical SUVR ≥ 1.5 [43] or the [^{18}F]Florbetapir PET cut-off of SUVR ≥ 1.10 [44], respectively. A side by side comparison of the three cohorts, including sample sizes, baseline cognitive diagnoses and studied outcomes in each cohort is offered in **Supplementary Table 4**.

2.2 Absolute IDQ p180 Kit Metabolite Measurements

Metabolites were measured with a targeted metabolomics approach using the AbsoluteIDQ® p180 Kit (BIOCRATES Life Science AG, Innsbruck, Austria), with a ultra-performance liquid chromatography (UPLC)/MS/MS system (Acquity UPLC (Waters), TQ-S triple quadrupole MS/MS (Waters)) which provides measurements of up to 186 endogenous metabolites quantitatively (amino acids and biogenic amines) and semi-quantitatively (acylcarnitines, sphingomyelins, PCs and lysoPCs across multiple classes) (see methods in **Supplementary Materials**). The AbsoluteIDQ® p180 kit has been fully

validated according to European Medicine Agency Guidelines on bioanalytical method validation. Additionally, plates include an automated technical validation to approve the validity of the run and provide verification of the actual performance of the applied quantitative procedure including instrumental analysis. The technical validation of each analyzed kit plate was performed using MetIDQ® software based on results obtained and defined acceptance criteria for blank, zero samples, calibration standards and curves, low/medium/high-level QC samples and measured signal intensity of internal standards over the plate. This is a highly useful platform that was used in hundreds of publications, including several studies in AD [11, 12, 15].

De-identified samples were analyzed following the manufacturer's protocol, with metabolomics labs blinded to diagnosis and pathological data. Serum samples from all 807 ADNI-1 participants were analyzed, but after QC, a smaller number of participants were included in the analysis (**Supplementary Figure 1**). Three participants were excluded due to incomplete clinical data, 70 samples were excluded due to non-fasting status, and 2 samples were excluded during the multivariate outlier detection step (see below), leaving 732 participants included in the final analyses. Each assay plate included two sets of replicates: 1) A set of duplicates obtained by pooling the first 72 samples in the study (QC pool duplicates), and 2) 20 blinded analytical duplicates (blinded duplicates).

2.3 P180 QC

Metabolites with >40% of measurements below the lower limit of detection (LOD) were excluded from the analysis. Metabolite values were scaled across the different plates using the QC pool duplicates. LOD values were imputed using each metabolite's LOD/2 value. Using the blinded duplicates, we selected metabolites with a coefficient of variation <20% and an intraclass correlation coefficient >0.65. Based on the QC process, 32 of the flow injection analysis (FIA) metabolites and 14 of the UPLC metabolites were excluded from further analysis (**Supplementary Table 5**). We checked for the presence of multivariate outlier participants by evaluating the first and second principal components in each platform. Two

multivariate outliers were beyond 7 standard deviations and were therefore excluded. For the participants with duplicated measurements, we used the average values of the two measured values in further analyses.

2.4 CSF $A\beta_{1-42}$ and Tau Biomarkers

Lumbar puncture was performed in the mornings after an overnight fast. $A\beta_{1-42}$, total tau (t-tau), and tau phosphorylated at threonine 181 (p-tau_{181}) were measured using the multiplex xMAP Luminex platform (Luminex Corp, Austin, TX) with Innogenetics immunoassay kit-based reagents (INNO-BIA AlzBio3; Ghent, Belgium; for research use-only reagents) (methods in **Supplementary Materials**) [45]. CSF samples were available and measured for 48.8% of the CN, 52% of the MCI and 54.9% of the AD participants. $A\beta_{1-42}$-defined groups were classified as normal or pathological based on the previously published concentration (192 pg/ml) [46].

2.5 Magnetic Resonance Imaging (MRI) Measures

1.5-T MRI non-accelerated sagittal volumetric 3D magnetization-prepared rapid gradient-echo MRI images were acquired at each performance site for the ADNI-1 participants (http://www.adni-info.org; http://adni.loni.usc.edu). Only images that passed QC evaluations were included. Cortical grey matter volumes were processed using the FreeSurfer version 4.4 image processing framework (http://surfer.nmr.mgh.harvard.edu/) [47]. Freesurfer ventricular volume of MRI scans that passed the QC was adjusted for total intracranial volume and used for longitudinal analyses. The Spatial Pattern of Abnormality for Recognition of Early Alzheimer's Disease (SPARE-AD), an index that captures brain atrophy related to AD and has shown association with AD CSF biomarker and clinical measures, and was calculated for the baseline visit of ADNI-1 participants, was assessed in the present analysis [48, 49].

2.6 Medication Adjustment

In the ADNI and IMAS cohort, 41 major medication classes used to treat psychiatric (including different categories of benzodiazepines, antipsychotics, and antidepressants) and cardiovascular conditions (including different categories of anti-hypertensives, cholesterol treatment, and anti-diabetics), as well as dietary supplements (Co-Q10, fish oil, nicotinic acid, and acetyl L-carnitine) were systematically coded and available for model-based evaluations of the influence of each drug type on metabolite levels (methods in **Supplementary Materials**). Intake of any medication within a category was coded as present or absent. Dose effect was not evaluated. The list of the studied medication categories and the percentage of subjects taking these medications in each of the diagnostic categories for the ADNI cohort is listed in **supplementary table 6**.

2.7 Statistical Analysis

Metabolites with a skewness>2 [50] that showed a departure of the normality distribution (D'Agostino test p-value<0.05) [50, 51] were $\log_{10}$ transformed to normalize their distribution. We implemented a two-stage regression approach, whereby metabolites were first adjusted for confounding medications and dietary supplements in a linear regression model. For each metabolite, medications were backward-selected via Bayesian information criteria (BIC) to select an optimal combination of medications for preventing confounding while limiting model complexity. One AD medication class, i.e. anti-cholinesterases, were excluded from this process due to highly significant correlations (Spearman's rho = 63,4%, P = 1.28×10^{-83}) of these medications with diagnosis (for details, see methods in **Supplementary Materials**). The residuals for each metabolite were then carried forward to test associations with clinical outcomes.

The cross-sectional association with categorical outcomes (clinical diagnosis and CSF $A\beta_{1-42}$ group) was studied using a logistic regression model. For the cross-sectional quantitative outcomes (t-tau/$A\beta_{1-42}$ ratio, SPARE-AD and ADAS-Cog 13), a linear regression model was applied. Age and gender were forced

covariates in all the models associating with clinical variables, and education was also forced into the models for ADAS-Cog 13 and clinical diagnosis, whereas *APOE* ε4 was backward-selected based on BIC for each outcome (see methods in **Supplementary Materials and Supplementary Table 7**). Diagnosis was not included as a covariate in the models in the primary analyses that studied $A\beta_{1-42}$, t-tau/$A\beta_{1-42}$ ratio, SPARE-AD and ADAS-Cog 13 associations. The p-values were Bonferroni corrected to adjust for multiple comparisons and a corrected 0.05 two-tailed p-value was considered significant. A Cox hazard model including age, gender, *APOE* ε4 presence, and education as covariates was used to evaluate the association of metabolite levels with progression from MCI to AD with a median follow-up of 3.0 years (IQR: 2.0-6.1). A mixed-effects model that included age, gender, education, *APOE* ε4 presence, time, and metabolite level as independent variables was used to study longitudinal associations between the metabolites and volumetric MRI changes (transformed to normalized distribution) during follow-up in the MCI participants (AD participants were excluded due to short follow-up) [52]. A mixed-effects model was also used to evaluate the association of metabolites with change in ADAS-Cog13 (transformed to normalized distribution) and included education as an additional covariate. Both models accounted for baseline cognitive and MRI measures for each participant. Median follow-up times for the MRI and cognitive analyses were 3.0 years (IQR: 2.0-5.0). An interaction with time was included in all mixed-effects models for the studied metabolites.

In the Rotterdam study, a linear regression model was fitted for the cross-sectional analysis with *g*-factor as the outcome and valine as the determinant, adjusting for age, gender, lipid lowering medication, and education. P-values and effect estimates of the significant metabolites are reported. [^{11}C]PiB PET analysis for IMAS samples included age, gender, and *APOE* ε4 presence, along with the $A\beta_{1-42}$ status on PET, as independent predictors of target metabolite measures using a linear regression model. All analyses were performed using the R software package [53].

2.7.1 Co-expression Network Construction and Module Analysis

We investigated the global baseline cross-sectional correlation structure of metabolites and their correlation with a subset of clinical and biomarker measures at baseline ($A\beta_{1-42}$, Tau/$A\beta_{1-42}$ ratio and ADAS-Cog13). We built the p180 co-expression network based on baseline-normalized data adjusted for age, education, gender, and *APOE* ε4 presence using the WGCNA R package [54].

2.7.2 Partial Correlation Analysis

Biochemically related metabolites and propagation patterns of effects on the clinical variables were investigated from a network perspective. A Gaussian graphical model (GGM) calculation was performed as described in Krumsiek et al. [55] using the GeneNet R package with default parameters. To illustrate effect propagation on clinical variables, we colored the resulting network similar to that in Mittelstrass et al. [56]. In brief, a GGM is an undirected graphical model based on partial correlation coefficients, i.e. pairwise correlation coefficients conditioned against correlations with all other included variables. GGMs, contrary to correlation networks, thus can reveal the direct relations between metabolites. To account for correlations between metabolites and clinical or other potentially predictive variables, we used metabolite residuals that accounted for effects of medication and dietary supplements (as described above) and additionally included age, gender, *APOE* ε4 presence, and education as covariates in the GGM generation process. To obtain significant partial correlations, we used a significance threshold of 0.05 after Bonferroni correction for all possible edges in the model ($0.05/10{,}296 = 4.86 \times 10^{-6}$). For each clinical variable, we colored the network representation of the GGM using the results of our regression analyses using sign(β)*(-log10(P)) to visualize both strength of association and direction of effect.

3. RESULTS

Metabolomic analyses were performed in the ADNI-1 cohort and key findings were further tested in the Rotterdam, EFR, and IMAS cohorts. Overall descriptions of sample size, composition and studied

outcomes across the different cohorts are shown in **Supplementary Table 4**. The results are presented for each cohort below.

3.1 ADNI-1 Cohort

In ADNI-1, CN, MCI, and AD participants did not differ in mean age, but as expected differed in *APOE* ε4 frequency, baseline cognition, MRI atrophy index, and CSF levels of T-tau and $A\beta_{1-42}$. The heatmap (**Figure 1**) (and the later described co-expression networks in **Supplementary Figure 2**) show that the global (i.e. direct and indirect) correlation structure between metabolites is formed into biochemical classes, illustrating that the metabolites with significant findings can be seen as proxies for the group of their correlating metabolites (**Supplementary Material File 2** presents the correlation values).

3.2 ADNI-1: Metabolites Associated With Cross-Sectional Clinical, MRI and CSF Biomarker Measures

The metabolites that remained in the analyses after the QC steps showed different correlation strengths, indicating groups of metabolites that may be involved in similar processes (**Figure 1**). After applying Bonferroni multiple comparison correction, 13 metabolites showed significant associations (Bonferroni adjusted p-value<0.05) with cognitive scores and CSF and MRI biomarker measures (**Table 1**). Six metabolites were associated with CSF $A\beta_{1-42}$ positivity (PC ae C36:2, PC ae C40:3, PC ae C42:4, PC ae C44:4, SM (OH) C14:1, SM C16:0), four were associated with t-tau/$A\beta_{1-42}$ ratio (C18, PC ae C36:2, SM C16:0, SM C20:2), five were associated with ADAS-Cog13 scores (C14:1, C16:1, SM C20:2, α-aminoadipic acid -α-AAA-, and valine), and 6 were associated with SPARE-AD scores (C12, C16:1, PC ae C42:4, PC ae C44:4, α-AAA and valine). In all analyses, higher acylcarnitine, PC, and SM values were associated with worse clinical and biomarker measures, whereas the opposite direction of associations was observed for valine and α–AAA values. The complete results for the 138 studied metabolites are listed in **Supplementary Table 8,** where many amines (including isoleucine, glutamate, tyrosine, tryptophan, glycine, proline, histidine, T4OH proline) and other metabolites within PC and SM classes showed significant non-comparison corrected associations with clinical markers and outcomes but

did not survive Bonferroni multiple comparison correction. **Supplementary Tables 9 and 10** present the analyses adjusted by clinical diagnosis and stratified by each of the three clinical diagnostic categories, respectively. All significant correlations were in the same directions in the clinical diagnostic groups.

We next evaluated differences in levels of key metabolites associated with cognitive or biomarker measures from the analyses reported above between the three diagnostic groups (CN, MCI, and AD) sub-classified by CSF $A\beta_{1-42}$ positivity status. Metabolites showed three different patterns of associations with the CSF AD biomarkers. PC ae C44:4, PC ae C36:2, and C18 represented the most significant examples of each of this patterns and the values in the six groups are shown in **Figure 2**. Of note, CN participants (red boxes) with pathological CSF $A\beta_{1-42}$ values showed significant metabolic changes in a specific group of metabolites when compared to CN with no pathological CSF $A\beta_{1-42}$ values (**Figure 2A**). Some of the changes associated with CSF $A\beta_{1-42}$ values appeared in clinical stages of disease (MCI and AD) (**Figure 2B**). Other metabolic changes were only observed in comparing CN participants to clinically impaired subjects (**Figure 2C**), but showed no associations with pathological CSF $A\beta_{1-42}$ status. **Figure 2D** illustrates valine correlation with cognition in the ADNI-1 study.

3.3 Metabolites Associated with Longitudinal Outcomes in the ADNI-1 Cohort

We evaluated whether levels of metabolites at baseline were associated with 1) ADAS-Cog13 changes up to 5 years; 2) ventricular volume changes up to 5 years; or 3) progression from MCI to AD (**Table 2**). Regression coefficients of six metabolites (PC ae C40:3, PC ae C42:4, PC ae C44:4, SM (OH) C14:1, SM C16:0 and SM C20:2) showed a positive association with all three longitudinal outcomes. In addition, the coefficients for valine and α–AAA were positively associated with cognitive decline, while the coefficient for valine was negatively associated with ventricular volume. **Figure 3** shows some of these associations as examples, including **Figure 3A** which shows the Cox hazards model of the association of SM C20:2 with conversion from MCI to AD, and **Figure 3B** which shows the association between baseline

concentration of SM 20:2 (presented as tertiles) and longitudinal cognitive (ADAS-Cog13) and MRI (brain ventricular volume) change.

3.4 Evaluation of Findings in the Rotterdam and ERF Studies

In the Rotterdam and ERF studies, only a subset of metabolites were measured from the panel of P180 metabolites evaluated in the ADNI-1 study (P150 panel, **Supplementary Table 11**). Using a targeted approach, we tested whether the metabolites that showed a significant association in the ADNI-1 study were also correlated with cognition (general cognitive ability: g-factor) in the Rotterdam Study or ERF. For the cross-sectional analysis, 8 metabolites were available in the ERF study. Two of these metabolites (PC ae C40:3, SM C20:2) were associated with cross-sectional general cognitive ability in the expected direction based on the discovery ADNI-1 cohort. Notice that higher general cognitive ability levels indicate better cognition as opposed to ADAS-Cog13. Valine was strongly associated with a higher general cognitive ability ($p=0.00035$) in the Rotterdam study (**Figure 2E**), which is in line with the association with ADAS-Cog13 in ADNI-1 (**Figure 2D**). Longitudinally, 342 participants developed AD in the Rotterdam study after a median follow-up time of 9.7 years (IQR 5.6-10.5). A Cox proportional hazard model was fitted adjusting for age at baseline, gender, education and lipid-lowering medication, and indicated that a one-SD increase in valine concentration was also associated with a decreased risk of AD ($p=0.044$).

3.5 Evaluation of $A\beta_{1-42}$ Signature in the IMAS Cohort

Three of the six metabolites (PC ae 42:4, PC ae 44:4 and SM(OH) C14:1) that showed an association with CSF $A\beta_{1-42}$ positivity in the ADNI-1 cohort were also associated with amyloid positivity on PET in the IMAS cohort (**Supplementary Table 12**) (n=34).

3.6 Partial Correlation Networks for $A\beta_{1-42}$, T-Tau, SPARE AD, ADAS-Cog13 – Metabolic Trajectory for Disease

We strived to define insights into the trajectory of biochemical changes that correlate with established models for disease [30], Aβ pathology, tau, imaging changes, and cognitive decline, building partial correlation networks for each clinical measure.

The partial correlation networks established direct connections between the measured metabolites, which have been shown to depict direct biochemical relationships between metabolites while omitting mediated correlations [55, 57]. **Figure 4** integrates the strength of the partial correlations between metabolites and overlays on these networks the associations with the studied outcomes $A\beta_{1-42}$, t-tau, SPARE-AD, and ADAS-Cog13 (partial correlation networks for p-tau and t-tau/$A\beta_{1-42}$ ratio are not shown). The networks showing the direct links between metabolites (nodes) identified through their strong partial correlations (edges) expand the heatmap information (**Figure 1**). Through coloring of the metabolite nodes by their association to CSF, imaging and cognitive markers, respectively (where bright colors indicate strong associations and blue and red color indicate up and down-regulation of metabolites), these networks demonstrate how the effects of clinical variables propagate along the edges within the network suggesting that the results follow biochemically plausible pathways. The studied outcomes cover the different stages of AD, matching known biomarkers of disease [30].

The network for $A\beta_{1-42}$ (**Figure 4A**) highlighted direct correlations with short- and medium-chain SMs and PC with ether-bonds, suggesting a role for membrane structure and function, contact sites, and membrane signaling in amyloid pathology. The correlation pattern for t-tau (**Figure 4B**) highlighted metabolites among long chain acylcarnitines and SMs implicated in lipid metabolism. The SPARE-AD and ADAS-Cog13 (**Figure 4B**) partial correlation networks were very similar, suggesting associations of brain atrophy and cognitive decline with metabolic changes in branched chain amino acids and short chain acylcarnitines implicated in mitochondrial energetics as well as additional changes in lipid metabolism.

3.7 Co-expression Network- Direct and Indirect Connections for Key Metabolites

The partial correlation networks above evaluated only direct connections among metabolites. To capture both indirect and direct correlations, we built co-expression networks to evaluate the number of modules in our dataset and evaluate additional connections between key metabolites identified as related to cognitive or biomarker measures in ADNI-1. The full co-expression network, which identified seven metabolic modules, can be found in **Supplementary Figure 2** and **Supplementary Material File 3** presents each of the individual correlations.

We investigated the correlation structure of the three metabolites in the ERF and Rotterdam datasets that significantly associated with cognition, namely PC ae C40:3, SM C20:2, valine as shown in **Figure 5**. The subnetwork shows these three metabolites to have high correlations (marked as red edges) to other functional metabolic modules via direct and indirect links. Valine was highly correlated with isoleucine and α-AAA, whereas SM C20:2 was highly correlated with a subset of the SMs including SM C16:0. Finally, PC ae C40:3 was highly correlated with PCs and SMs, but not amines and acylcarnitines. These SMs and PCs were significantly associated with cognitive scores, CSF biomarkers and MRI measures (**Table 1**).

4. DISCUSSION

The Alzheimer Disease Metabolomics Consortium (ADMC) funded by the NIA under the AMP-AD and MOVE-AD initiatives and in partnership with ADNI has as its goal to create a comprehensive metabolomics database for AD. This data will fill in biochemical knowledge about disease mechanisms that can be used as a roadmap for novel drug discovery and establishment of blood-based biomarkers. Eight complementary, targeted and non-targeted, metabolomics platforms are currently in the process of generating data on ADNI participants to define the metabolic trajectory of disease connecting central and peripheral metabolic failures in a pathway and network context. We seek to replicate earlier findings and test hypotheses, but also expand on biochemical coverage to better understand disease pathogenesis by using complementary data unique to ADNI-1. The unique opportunity of having longitudinal cognitive and imaging data on each subject for close to a decade enables identification of peripheral biomarkers that are disease related.

This is the first report from ADMC on use of a targeted, highly validated metabolomics platform with the analysis guided by CSF markers and imaging data. Using 732 baseline serum samples from the ADNI-1 cohort, we systematically evaluated the relationships between metabolomics data and cross-sectional clinical, CSF, and MRI measures, as well as their association with longitudinal cognitive and brain volume changes. We demonstrate a novel approach to the analysis of neurodegenerative disease mechanisms. Multiple comparisons and covariate-adjusted analyses, that included relevant medications, identified sets of metabolites that became altered at specific disease stages (preclinical AD with biomarker-defined AD pathology vs symptomatic stages) [30]. Using partial correlation networks we integrate our findings of metabolic effects on AD pathogenesis, linking central and peripheral metabolism in a way that consistently reconciles biochemical trajectories of disease with this established temporal sequence of pathophysiological stages of AD. In the following, we therefore discuss our findings in their temporal order along AD pathogenesis.

Aβ pathology

Changes observed earliest in AD, namely in biomarker-defined preclinical stages [58] in CN participants, were higher levels of a specific set of PCs (PC ae C36.2, PC ae C40.3, PC ae C42.4, and PC ae C44.4) and SMs (SM (OH) C14.1, SM C16.0). These metabolites were associated with abnormal CSF $A\beta_{1-42}$ values in CN participants to a similar degree as observed in MCI, indicating an early role of ether-containing PC species and SM in the development of the disease. Interestingly, most of these metabolites were also associated with later cognitive decline and global brain atrophy changes in the MCI group (**Table 1**). The use of information on AD CSF biomarkers was extremely useful and guided our metabolomics data . Only after sub-stratification of the diagnostic groups (CN, MCI and AD) based on CSF biomarkers were we able to detect the increased values of these metabolites in participants with CSF pathology stressing the importance of using biomarkers to detect early biochemical changes [59]. Our findings along with those of several others [11, 15] all point to problems with phospholipid metabolism that happen early in the disease process. These early changes by themselves are not sufficient predictors of disease or progression but they might provide extremely valuable mechanistic insights.

Partial correlation networks showed that the pathological CSF $A\beta_{1-42}$ values were associated with two groups of lipids, composed primarily of ether-containing PCs and relatively short-chain SMs. Ether-containing PC (PC ae) metabolites are PC species with an ether linkage of an aliphatic chain to the first hydroxyl position of glycerol. These lipids are not completely characterized and may represent a mixture of lipid metabolites including plasmalogens, acyl-alkyl PC or PC containing an odd-numbered fatty acyl chain. When measured in the serum, the ether-containing lipids are derived from liver metabolism and are possible indicators of peroxisomal function and lipid oxidation status [60, 61]. Plasmalogens and SMs are enriched in membrane rafts where they facilitate signal transduction and serve as a source for lipid secondary messengers [62]. The association of PCs and SMs in our study and others [14, 63] with early changes in AD and with pathological CSF $A\beta_{1-42}$ levels (**Figures 4B and 5**) may be indicative of early

neurodegeneration and loss of membrane function. Ether-linked PC metabolites are found in high abundance in plasma membranes, and are a source for signaling molecules [64], particularly platelet activating factor and arachidonic acid. Similarly, they are found in high abundance in immune cells, are regulatory factors, and may be part of the link between inflammation and AD [65]. Both SMs and ether-linked PCs may be located in membrane rafts, supporting the hypothesis that lipid rafts are directly associated with regulation of amyloid precursor protein processing, the production of $A\beta_{1-42}$, and facilitate its aggregation [66]. All of these lipid biological functions related to $A\beta_{1-42}$ might provide great insight about mechanisms of $A\beta_{1-42}$ pathology, but at this early stage, we cannot assign cause or effect. Because this study was conducted using peripheral blood, we cannot directly associate the changes in neuronal lipid rafts with changes in signaling and accumulation of cerebral $A\beta_{1-42}$.

Previous smaller studies relying on clinical measures identified only associations between these metabolite categories and dementia diagnosis or clinical progression [12, 15, 67], indicating that these metabolic pathways may contribute significantly to AD pathophysiology. Differences in the specific metabolites identified in the published studies [12, 15, 67] may be due to differences in sample selection criteria, disease severity or for the absence or presence of controlling for different confounders in the data analysis.

Tau pathology

In this study, pathological CSF $A\beta_{1-42}$ shows an association with ether-linked PC, and shorter chain SM, but not amines, lysoPC, or acylcarnitines. $A\beta_{1-42}$ changes happen early in disease, followed by accumulation of tau protein in the CSF [30]. In our analysis, tau related metabolites were very different both from those that correlate with $A\beta_{1-42}$ as well as from metabolites associated with brain atrophy and cognitive changes. Tau related metabolites thus appear to belong to an intermediate stage between $A\beta_{1-42}$

accumulation and changes in imaging and cognitive function (**Figures 4B**), further supporting our hypothesis that different metabolic events occur at different disease stages.

Long-chain acylcarnitines, PC ae C36:2, and SM.C20:2 were higher only in cognitively impaired participants with AD-like CSF $A\beta_{1-42}$ values, indicating that changes in these metabolites are more specific to AD-related neurodegeneration reflecting possible changes in multiple cellular processes. Specifically, accumulation of acylcarnitine species containing long fatty acyl chains indicates malfunction of fatty acid transport and/or β-oxidation in mitochondria, inefficient utilization of fatty acids as energy substrates [68] or alterations in tau metabolism [69]. In the current study, we revealed that the levels of several acylcarnitine species were increased either at the MCI stage or in clinical AD [70] (**Table 1**). Acylcarnitines have important functions in the brain [70] such as mitochondrial function, energetics, and neurotransmission that need to be further explored and connected to peripheral function.

Brain volume changes and cognitive decline

In our study, partial correlation networks show a pattern of inverse associations between brain volume changes (measured by SPARE-AD) and cognition (ADAS-Cog 13) and long and short acylcarnitines, valine, and α-AAA, indicating a shift in energy substrate utilization in later stages of AD (**Figure 4**). By using a second type of networking analysis, a co-expression network, our data show the relationship between valine and short acylcarnitines (**Figure 5, dark green cluster**), reinforcing the hypothesized changes in energetics. The association of the long chain acylcarnitines, odd-numbered acylcarnitines and amino acids in relation with ADAS-Cog scores, supports a switch of utilization from fatty acids to amino acids and glucose. In the network analysis, the amines and short-chain acylcarnitines did not link to PCs and SMs, rather they clustered together in smaller groups. This may indicate that the short chain acylcarnitines are associated in energy and amino acid metabolism rather than lipid metabolism in AD participants. This novel finding indicates a disease-associated transition in pathways for utilization of

energy substrates. Whether such a switch is associated specifically with AD pathogenesis or is a function of aging [71] remains to be tested. Interestingly, ADAS-Cog13 does not show the associations with SMs or ether-linked PCs found with pathological CSF $A\beta_{1-42}$. Therefore, it is possible that metabolic pathways other than those associated with lipid rafts are dysregulated later in the disease process.

It is not clear if insulin resistance is a cause, an effect or some combination of cause and effect in AD [72]. Insulin resistance, obesity, and diabetes are risk factors for AD [73], with lipid metabolism disorder (and inflammation) being a common link between metabolic disease, vascular disease, and AD. Several ether-linked PC metabolites have been associated with the risk of diabetes [74], insulin resistance promotes aminoacidaemia and the use of amino acids for energy [68], and BCAA and α-AAA have been identified as predicting diabetes risk [75, 76]. BCAAs (valine, leucine and isoleucine) play central roles in metabolism and have been implicated in insulin resistance, type 2 diabetes mellitus (T2DM) and obesity. Our findings in ADNI related to low levels of valine and its correlation with cognitive changes were confirmed in the large Rotterdam study, pointing to an important role for this BCAA in cognitive changes in AD. Low levels of BCAAs have been implicated in hepatic insulin resistance in liver disease and may have a broader role in insulin resistance in the brain [77]. The seemingly paradoxical directionality difference in correlation of BCAAs with diabetes and cognition needs to be further evaluated in longitudinal studies taking into account weight changes, tissue type and differences in human and animal model systems [28, 78]. Our understanding of the biochemical crossroads between diabetes and AD could be greatly enhanced by metabolic profiling of both central and peripheral tissues in both diseases and over time.

Concluding remarks

In summary, by using metabolomics and network approaches this study has revealed lipid metabolic changes related to early stages of disease, as well as later changes related to mitochondrial energetics and

energy utilization. We hypothesize that the lipid changes measured in this study reflect alterations in membrane structure and function early in the disease process, and suggest a change in lipid rafts, which in turn, cause alterations in Aβ processing [66]. We hypothesize that over time, the changes in lipid membranes, particularly mitochondrial membranes results in increased lipid oxidation, loss of membrane potential, and changes in membrane transport [79, 80]. All of these lipid membrane changes might be reflected as disruption in BCAA as an energy source, production of acylcarnitines and altered energy substrate utilization. The link between the altered energy metabolism, glycolysis, use of ketone bodies, and development of insulin resistance are all subject of ongoing longitudinal studies using complementary metabolomics platforms that enable the study of those biochemical pathways. The specific interactions between the peripheral metabolic network changes, central changes and the timeline of AD pathophysiology reveal that peripheral metabolic changes can impact long-term brain health and function. This study thus provides an approach to define viable disease biomarkers based on understanding of whole-body AD pathophysiology at a systems level.

Previous studies have shown seemingly conflicting results regarding the diagnostic and prognostic classification of metabolomics data in AD [11, 15]. Our findings show that using a network approach many of these findings might be related such as early changes in phospholipid metabolism. Large meta analysis across many metabolomics studies using our network approaches is ongoing
By using the unique data available as part of ADNI, we were able to establish robust associations accounting for several confounders that lead to a better understanding of metabolic changes present in AD. Gender showed the strongest associations with many metabolites, but also age, BMI and several medications and food supplements, like statins and fish oils, had significant effects on several metabolites. The fact that medication use varied among the groups (for example fish oil intake was more frequent in CN and MCI subjects while use of SSRIs was lower in CN subjects), and that sometimes studied groups are unbalanced in terms of demographics makes it imperative to account for all possible confounders. Our results thus suggest that future studies should account for associations of metabolites

with both gender and medications. This is an important outcome, as prior studies have failed to address effects of medications on the metabolome; a limitation that can cause misleading conclusions. Many of the drugs used by AD patients were shown to have profound effects on metabolism (for reviews on drug effects see Kaddurah-Daouk and Weinshilboum [8, 9]). A detailed analysis of medications as confounds and meta-analysis of previously reported metabolomics studies addressing confounds will be published separately.

Limitations of our study are several. At this early stage, we cannot determine which of the metabolic changes we see are causative and which are a consequence of disease. Future mechanistic studies in model systems are needed to test hypothesis generated along with building of predictive metabolic networks. Gender metabolic differences are clear from this dataset and although adjusted for in this study ongoing analysis and modeling of gender differences will be key. Profiling blood samples across the trajectory of disease will provide valuable information and is currently on going. In addition, analysis of CN cohort with normal CSF $A\beta_{1-42}$ values will be useful to evaluate within subject variability. Linking peripheral and central metabolic changes in blood, CSF and brain tissue is critical for better defining peripheral influences like diet and environment on brain health and disease. The effect of confounds like medications impacts metabolomics findings in significant ways and must be addressed carefully. In our study, we had medication data for two of the cohort (ADNI and IMAS), but this information was not available for the Rotterdam and ERF studies. Therefore, there are differences in how the data was processed across cohorts. Finally, neuropsychological assessments evaluated in the ADNI and Rotterdam and ERF scores were not the same. ADNI analyses were based on a global cognitive scale, whereas in the Rotterdam and ERF studies a composite measure, the g-factor. Therefore, these scales might differently represent the summary of the diverse cognitive functions.

Over the past decade we have gained significant knowledge about effects of commonly used medications and have tried to address their confounds in studies like ADNI. More sophisticated modeling approaches will be needed to address complex interactions with medications so this study presents early effort. Defining genetic factors that influence metabolic changes is key and is ongoing. Broad biochemical coverage is needed to better define mechanism and trajectory of disease. The ADMC is producing metabolomics datasets from eight targeted and non-targeted platforms on the large ADNI cohort. After these and other cohort datasets are available, we look forward to working with the international scientific community to build a comprehensive model for AD using integrated multi-omic network approaches.

.

ACKNOWLEDGEMENTS

National Institute on Aging [R01AG046171, RF1AG051550 and 3U01AG024904-09S4] supported the Alzheimer Disease Metabolomics Consortium. JBT is supported by National Institute on Aging [R01AG046171, RF1AG051550, and P50 NS053488]. AJS is additionally supported by NIA R01 AG19771, NIA P30 AG10133 and NLM R01 LM011360 JQT is additionally supported by National Institute on Aging [P30 AG10124] in the conduct of ADNI-1 data analyses. MA was supported by the Helmholtz cross-program topic "Metabolic Dysfunction". KN was additionally supported by National Library of Medicine [R00 LM011384]. LS was additionally supported by National Library of Medicine [R01 LM011360] and National Institute of Biomedical Imaging and Bioengineering [R01 EB022574]. SLR was additionally supported by National Institute on Aging K01 AG049050, the Alzheimer's Association, the Indiana Clinical and Translational Science Institute, and the Indiana University-IU Health Strategic Neuroscience Research Initiative. KS was supported by 'Biomedical Research Program' funds at Weill Cornell Medical College in Qatar, a program funded by the Qatar Foundation Data collection and sharing for this project was funded by the ADNI (National Institutes of Health Grant U01 AG024904) and DOD ADNI (Department of Defense award number W81XWH-12-2-0012). ADNI is funded by the National Institute on Aging, the National Institute of Biomedical Imaging and Bioengineering, and through generous contributions from the following: Alzheimer's Association; Alzheimer's Drug Discovery Foundation; Araclon Biotech; BioClinica, Inc.; Biogen Idec Inc.; Bristol-Myers Squibb Company; Eisai Inc.; Elan Pharmaceuticals, Inc.; Eli Lilly and Company; EuroImmun; F. Hoffmann-La Roche Ltd and its affiliated company Genentech, Inc.; Fujirebio; GE Healthcare; IXICO Ltd.; Janssen Alzheimer Immunotherapy Research & Development, LLC.; Johnson & Johnson Pharmaceutical Research & Development LLC.; Medpace, Inc.; Merck & Co., Inc.; Meso Scale Diagnostics, LLC.; NeuroRx Research; Neurotrack Technologies; Novartis Pharmaceuticals Corporation; Pfizer Inc.; Piramal Imaging; Servier; Synarc Inc.; and Takeda Pharmaceutical Company. The Canadian Institutes Health Research is providing funds to support ADNI clinical sites in Canada. Private sector contributions are facilitated by the Foundation for the National Institutes of Health (www.fnih.org). The

grantee organization is the Northern California Institute for Research and Education, and the study is coordinated by the Alzheimer's Disease Cooperative Study at the University of California, San Diego. ADNI data are disseminated by the Laboratory for Neuro Imaging at the University of Southern California. The Alzheimer Metabolomics consortium is a part of NIA national initiatives AMP-AD and M^2OVE AD.

Erasmus Rucphen Family study (ERF)

The ERF study was approved by the Medical Ethics Committee of the Erasmus MC. The committee is constituted according to the WMO (National act medical-scientific research in human beings). A written informed consent was obtained from all study participants. The ERF study as a part of EUROSPAN (European Special Populations Research Network) was supported by European Commission FP6 STRP grant number 018947 (LSHG-CT-2006-01947) and also received funding from the European Community's Seventh Framework Program (FP7/2007-2013)/grant agreement HEALTH-F4-2007-201413 by the European Commission under the program "Quality of Life and Management of the Living Resources" of 5th Framework Program (no. QLG2-CT-2002-01254). The ERF study was further supported by ENGAGE consortium and CMSB. High-throughput analysis of the ERF data was supported by joint grant from Netherlands Organization for Scientific Research and the Russian Foundation for Basic Research (NWO-RFBR 047.017.043). We are grateful to all study participants and their relatives, general practitioners and neurologists for their contributions and to P. Veraart for her help in genealogy, J. Vergeer for the supervision of the laboratory work.

Rotterdam Study (RS)

The Rotterdam Study has been approved by the Medical Ethics Committee of the Erasmus MC and by the Ministry of Health, Welfare and Sport of the Netherland , implementing the Wet Bevolkingsonderzoek: ERGO (Population Studies Act: Rotterdam Study). All participants provided written informed consent to participate in the study and to obtain information from their treating physicians. The Rotterdam Study is

supported by the Erasmus MC University Medical Center and Erasmus University Rotterdam; The Netherlands Organisation for Scientific Research (NWO); The Netherlands Organisation for Health Research and Development (ZonMw); the Research Institute for Diseases in the Elderly (RIDE); The Netherlands Genomics Initiative (NGI); the Ministry of Education, Culture and Science; the Ministry of Health, Welfare and Sports; the European Commission (DG XII); and the Municipality of Rotterdam. The contribution of inhabitants, general practitioners and pharmacists of the Ommoord district to the Rotterdam Study is gratefully acknowledged. Ayse Demirkan is supported by a Veni grant (2015) from ZonMw.

The study sponsors had no role in the study design, the collection, analysis and interpretation of data, the writing of the report, or the decision to submit the article for publication.

DISCLOSURES

JBT reports investigator-initiated research support from Eli Lilly unrelated to the work reported here.

MA, GM, RC, RB, XH, MT, JDT, KS, JWT, LSW, SMD, DR, JJ, AMR, SLR, CB, GL,…SK, KN, LS, RC, SV, CLQ, MAM, KZ, MH, SVL, ACH, AD, TH, and CMD report no disclosures.

HZ is salaried employee of Sanofi.

GD, KK, TK are employed by Biocrates Life Sciences AG. These authors have no other financial relationships relevant to this article to disclose.

JQT may accrue revenue in the future on patents submitted by the University of Pennsylvania wherein he is co-Inventor and he received revenue from the sale of Avid to Eli Lily as co-inventor on imaging related patents submitted by the University of Pennsylvania.

LMS receives research funding from: NIH (U01 AG024904; R01 MH 098260; R01 AG 046171; 1RF AG 051550); MJFox Foundation for PD Research (BioFIND) and is a consultant for: Eli Lilly; Novartis; Roche; he provides QC oversight for the AlzBio3 immunoassay (Fujirebio) and for the Roche Elecsys immunoassay as part of responsibilities for the ADNI study.

AJS reports investigator-initiated research support from Eli Lilly unrelated to the work reported here. He has received consulting fees and travel expenses from Eli Lilly and Siemens Healthcare and is a consultant to Arkley BioTek. He also receives support from Springer publishing as Editor in chief of Brain Imaging and Behavior.

MWW reports stock/stock options from Elan, Synarc, travel expenses from Novartis, Tohoku University, Fundacio Ace, Travel eDreams, MCI Group, NSAS, Danone Trading, ANT Congress, NeuroVigil, CHRU-Hopital Roger Salengro, Siemens, AstraZeneca, Geneva University Hospitals, Lilly, University of California, San Diego–ADNI, Paris University, Institut Catala de Neurociencies Aplicades, University of New Mexico School of Medicine, Ipsen, Clinical Trials on Alzheimer's Disease, Pfizer, AD PD meeting, PMD has received advisory fees from Avid/Lilly, Anthrotonix, Muses Labs, AstraZeneca, Abbvie, Baxter, Cognoptix, Lundbeck/Takeda, Piramal, Genomind, Sonexa, Targacept, Danone, Neurocog Trials, EnVivo, T3D Therapeutics. PMD has received research grants (through Duke University) from Elan, Avid/Lilly, Janssen, Pfizer/Medivation, Neuronetrix, Forum, Alzheimer's Drug Discovery Foundation. PMD has received fees for lecture from Lundbeck and Alzheimer's Association, and for developing educational materials from Physicians Postgraduate Press. PMD owns shares or options in Maxwell Health, Muses Labs, Anthrotronix, Evidation, Turtle Shell Technologies and Advera Health Analytics whose products are not discussed here. PMD has received travel funds from Biogen. He is a coinventor on a use patent for metabolomics in Alzheimer's (through Duke University) that is unlicensed and he receives no royalties on this.

RKD inventor on key patents in the field of metabolomics including applications for Alzheimer disease.

REFERENCES

[1] Citron M. Alzheimer's disease: strategies for disease modification. Nature reviews Drug discovery. 2010;9:387-98.

[2] Cai H, Cong WN, Ji S, Rothman S, Maudsley S, Martin B. Metabolic dysfunction in Alzheimer's disease and related neurodegenerative disorders. Current Alzheimer research. 2012;9:5-17.

[3] de la Monte SM, Tong M. Brain metabolic dysfunction at the core of Alzheimer's disease. Biochemical pharmacology. 2014;88:548-59.

[4] Procaccini C, Santopaolo M, Faicchia D, Colamatteo A, Formisano L, de Candia P, et al. Role of metabolism in neurodegenerative disorders.

[5] Chen Z, Zhong C. Decoding Alzheimer's disease from perturbed cerebral glucose metabolism: implications for diagnostic and therapeutic strategies. Progress in neurobiology. 2013;108:21-43.

[6] Patti GJ, Yanes O, Siuzdak G. Innovation: Metabolomics: the apogee of the omics trilogy. Nature reviews Molecular cell biology. 2012;13:263-9.

[7] Kaddurah-Daouk R, Krishnan KR. Metabolomics: a global biochemical approach to the study of central nervous system diseases. Neuropsychopharmacology : official publication of the American College of Neuropsychopharmacology. 2009;34:173-86.

[8] Kaddurah-Daouk R, Weinshilboum R. Metabolomic Signatures for Drug Response Phenotypes: Pharmacometabolomics Enables Precision Medicine. Clinical pharmacology and therapeutics. 2015;98:71-5.

[9] Kaddurah-Daouk R, Weinshilboum RM. Pharmacometabolomics: implications for clinical pharmacology and systems pharmacology. Clinical pharmacology and therapeutics. 2014;95:154-67.

[10] Han X, Rozen S, Boyle SH, Hellegers C, Cheng H, Burke JR, et al. Metabolomics in early Alzheimer's disease: identification of altered plasma sphingolipidome using shotgun lipidomics. PloS one. 2011;6:e21643.

[11] Casanova R, Varma S, Simpson B, Kim M, An Y, Saldana S, et al. Blood metabolite markers of preclinical Alzheimer's disease in two longitudinally followed cohorts of older individuals. Alzheimer's & dementia : the journal of the Alzheimer's Association. 2016.

[12] Fiandaca MS, Zhong X, Cheema AK, Orquiza MH, Chidambaram S, Tan MT, et al. Plasma 24-metabolite Panel Predicts Preclinical Transition to Clinical Stages of Alzheimer's Disease. Frontiers in neurology. 2015;6:237.

[13] Klavins K, Koal T, Dallmann G, Marksteiner J, Kemmler G, Humpel C. The ratio of phosphatidylcholines to lysophosphatidylcholines in plasma differentiates healthy controls from patients with Alzheimer's disease and mild cognitive impairment. Alzheimer's & dementia (Amsterdam, Netherlands). 2015;1:295-302.

[14] Koal T, Klavins K, Seppi D, Kemmler G, Humpel C. Sphingomyelin SM(d18:1/18:0) is significantly enhanced in cerebrospinal fluid samples dichotomized by pathological amyloid-beta42, tau, and phospho-tau-181 levels. J Alzheimers Dis. 2015;44:1193-201.

[15] Mapstone M, Cheema AK, Fiandaca MS, Zhong X, Mhyre TR, MacArthur LH, et al. Plasma phospholipids identify antecedent memory impairment in older adults. Nature medicine. 2014;20:415-8.

[16] Motsinger-Reif AA, Zhu H, Kling MA, Matson W, Sharma S, Fiehn O, et al. Comparing metabolomic and pathologic biomarkers alone and in combination for discriminating Alzheimer's disease from normal cognitive aging. Acta neuropathologica communications. 2013;1:28.

[17] Kaddurah-Daouk R, Rozen S, Matson W, Han X, Hulette CM, Burke JR, et al. Metabolomic changes in autopsy-confirmed Alzheimer's disease. Alzheimer's & dementia : the journal of the Alzheimer's Association. 2011;7:309-17.

[18] Kaddurah-Daouk R, Zhu H, Sharma S, Bogdanov M, Rozen SG, Matson W, et al. Alterations in metabolic pathways and networks in Alzheimer's disease. Translational psychiatry. 2013;3:e244.

[19] Gonzalez-Dominguez R, Garcia-Barrera T, Vitorica J, Gomez-Ariza JL. Metabolomic investigation of systemic manifestations associated with Alzheimer's disease in the APP/PS1 transgenic mouse model. Mol Biosyst. 2015;11:2429-40.
[20] Soltow QA, Jones Dp Fau - Promislow DEL, Promislow DE. A network perspective on metabolism and aging.
[21] Simpson BN, Kim M, Chuang YF, Beason-Held L, Kitner-Triolo M, Kraut M, et al. Blood metabolite markers of cognitive performance and brain function in aging. Journal of cerebral blood flow and metabolism : official journal of the International Society of Cerebral Blood Flow and Metabolism. 2015.
[22] Han X, Holtzman DM, McKeel DW, Jr. Plasmalogen deficiency in early Alzheimer's disease subjects and in animal models: molecular characterization using electrospray ionization mass spectrometry. Journal of neurochemistry. 2001;77:1168-80.
[23] Wood PL, Smith T Fau - Lane N, Lane N Fau - Khan MA, Khan Ma Fau - Ehrmantraut G, Ehrmantraut G Fau - Goodenowe DB, Goodenowe DB. Oral bioavailability of the ether lipid plasmalogen precursor, PPI-1011, in the rabbit: a new therapeutic strategy for Alzheimer's disease.
[24] Ibanez C, Simo C, Martin-Alvarez PJ, Kivipelto M, Winblad B, Cedazo-Minguez A, et al. Toward a predictive model of Alzheimer's disease progression using capillary electrophoresis-mass spectrometry metabolomics. Analytical chemistry. 2012;84:8532-40.
[25] Trushina E, Dutta T, Persson XM, Mielke MM, Petersen RC. Identification of altered metabolic pathways in plasma and CSF in mild cognitive impairment and Alzheimer's disease using metabolomics. PloS one. 2013;8:e63644.
[26] Li D, Misialek JR, Boerwinkle E, Gottesman RF, Sharrett AR, Mosley TH, et al. Plasma phospholipids and prevalence of mild cognitive impairment and/or dementia in the ARIC Neurocognitive Study (ARIC-NCS). Alzheimer's & dementia (Amsterdam, Netherlands). 2016;3:73-82.
[27] Savica R, Murray ME, Persson XM, Kantarci K, Parisi JE, Dickson DW, et al. Plasma sphingolipid changes with autopsy-confirmed Lewy Body or Alzheimer's pathology. Alzheimer's & dementia (Amsterdam, Netherlands). 2016;3:43-50.
[28] Pan X, Nasaruddin MB, Elliott CT, McGuinness B, Passmore AP, Kehoe PG, et al. Alzheimer's disease-like pathology has transient effects on the brain and blood metabolome. Neurobiol Aging. 2016;38:151-63.
[29] Santiago JA, Potashkin JA. A network approach to clinical intervention in neurodegenerative diseases. Trends in molecular medicine. 2014;20:694-703.
[30] Jack CR, Jr., Holtzman DM. Biomarker modeling of Alzheimer's disease. Neuron. 2013;80:1347-58.
[31] Weiner MW, Veitch DP, Aisen PS, Beckett LA, Cairns NJ, Cedarbaum J, et al. Impact of the Alzheimer's Disease Neuroimaging Initiative, 2004 to 2014. Alzheimer's & dementia : the journal of the Alzheimer's Association. 2015;11:865-84.
[32] Draisma HH, Pool R, Kobl M, Jansen R, Petersen AK, Vaarhorst AA, et al. Genome-wide association study identifies novel genetic variants contributing to variation in blood metabolite levels. Nat Commun. 2015;6:7208.
[33] Wurtz P, Havulinna AS, Soininen P, Tynkkynen T, Prieto-Merino D, Tillin T, et al. Metabolite profiling and cardiovascular event risk: a prospective study of 3 population-based cohorts. Circulation. 2015;131:774-85.
[34] Ikram MA, van der Lugt A, Niessen WJ, Koudstaal PJ, Krestin GP, Hofman A, et al. The Rotterdam Scan Study: design update 2016 and main findings. Eur J Epidemiol. 2015;30:1299-315.
[35] Liu F, Pardo LM, Schuur M, Sanchez-Juan P, Isaacs A, Sleegers K, et al. The apolipoprotein E gene and its age-specific effects on cognitive function. Neurobiol Aging. 2010;31:1831-3.
[36] Hoogendam YY, Hofman A, van der Geest JN, van der Lugt A, Ikram MA. Patterns of cognitive function in aging: the Rotterdam Study. Eur J Epidemiol. 2014;29:133-40.

[37] de Bruijn RF, Bos MJ, Portegies ML, Hofman A, Franco OH, Koudstaal PJ, et al. The potential for prevention of dementia across two decades: the prospective, population-based Rotterdam Study. BMC Med. 2015;13:132.
[38] Davies G, Armstrong N, Bis JC, Bressler J, Chouraki V, Giddaluru S, et al. Genetic contributions to variation in general cognitive function: a meta-analysis of genome-wide association studies in the CHARGE consortium (N=53949). Mol Psychiatry. 2015;20:183-92.
[39] Risacher SL, Wudunn D, Pepin SM, MaGee TR, McDonald BC, Flashman LA, et al. Visual contrast sensitivity in Alzheimer's disease, mild cognitive impairment, and older adults with cognitive complaints. Neurobiol Aging. 2013;34:1133-44.
[40] Wang Y, Risacher SL, West JD, McDonald BC, Magee TR, Farlow MR, et al. Altered default mode network connectivity in older adults with cognitive complaints and amnestic mild cognitive impairment. J Alzheimers Dis. 2013;35:751-60.
[41] Kim S, Swaminathan S, Inlow M, Risacher SL, Nho K, Shen L, et al. Influence of genetic variation on plasma protein levels in older adults using a multi-analyte panel. PloS one. 2013;8:e70269.
[42] Ramanan VK, Risacher SL, Nho K, Kim S, Shen L, McDonald BC, et al. GWAS of longitudinal amyloid accumulation on 18F-florbetapir PET in Alzheimer's disease implicates microglial activation gene IL1RAP. Brain. 2015;138:3076-88.
[43] Klunk WE, Engler H, Nordberg A, Wang Y, Blomqvist G, Holt DP, et al. Imaging brain amyloid in Alzheimer's disease with Pittsburgh Compound-B. Annals of neurology. 2004;55:306-19.
[44] Landau SM, Breault C, Joshi AD, Pontecorvo M, Mathis CA, Jagust WJ, et al. Amyloid-beta imaging with Pittsburgh compound B and florbetapir: comparing radiotracers and quantification methods. Journal of nuclear medicine : official publication, Society of Nuclear Medicine. 2013;54:70-7.
[45] Kang JH, Korecka M, Figurski MJ, Toledo JB, Blennow K, Zetterberg H, et al. The Alzheimer's Disease Neuroimaging Initiative 2 Biomarker Core: A review of progress and plans. Alzheimer's & dementia : the journal of the Alzheimer's Association. 2015;11:772-91.
[46] Shaw LM, Vanderstichele H, Knapik-Czajka M, Clark CM, Aisen PS, Petersen RC, et al. Cerebrospinal fluid biomarker signature in Alzheimer's disease neuroimaging initiative subjects. Annals of neurology. 2009;65:403-13.
[47] Reuter M, Schmansky NJ, Rosas HD, Fischl B. Within-subject template estimation for unbiased longitudinal image analysis. NeuroImage. 2012;61:1402-18.
[48] Fan Y, Shen D, Gur RC, Gur RE, Davatzikos C. COMPARE: classification of morphological patterns using adaptive regional elements. IEEE transactions on medical imaging. 2007;26:93-105.
[49] Toledo JB, Da X, Bhatt P, Wolk DA, Arnold SE, Shaw LM, et al. Relationship between plasma analytes and SPARE-AD defined brain atrophy patterns in ADNI. PloS one. 2013;8:e55531.
[50] Rmetrics Core Team DW, Tobias Setz and Yohan Chalabi fBasics: Rmetrics - Markets and Basic Statistics. R package version. 2014.
[51] D'Agostino R.B. PES. Tests for Departure from Normality. Biometrika. 1973;60: 613–22.
[52] Pinheiro JC, Bates DM. Mixed-Effects Models in S and S-PLUS. New York: Springer Verlag; 2000.
[53] R Core Team. R: A Language and Environment for Statistical Computing. Vienna, Austria: R Foundation for Statistical Computing; 2015.
[54] Langfelder P, Horvath S. WGCNA: an R package for weighted correlation network analysis. BMC bioinformatics. 2008;9:559.
[55] Krumsiek J, Suhre K, Illig T, Adamski J, Theis FJ. Gaussian graphical modeling reconstructs pathway reactions from high-throughput metabolomics data. BMC systems biology. 2011;5:21.
[56] Mittelstrass K, Ried JS, Yu Z, Krumsiek J, Gieger C, Prehn C, et al. Discovery of sexual dimorphisms in metabolic and genetic biomarkers. PLoS genetics. 2011;7:e1002215.

[57] Krumsiek J, Suhre K, Evans AM, Mitchell MW, Mohney RP, Milburn MV, et al. Mining the unknown: a systems approach to metabolite identification combining genetic and metabolic information. PLoS genetics. 2012;8:e1003005.
[58] Jack CR, Jr., Albert MS, Knopman DS, McKhann GM, Sperling RA, Carrillo MC, et al. Introduction to the recommendations from the National Institute on Aging-Alzheimer's Association workgroups on diagnostic guidelines for Alzheimer's disease. Alzheimer's & dementia : the journal of the Alzheimer's Association. 2011;7:257-62.
[59] Toledo JB, Brettschneider J, Grossman M, Arnold SE, Hu WT, Xie SX, et al. CSF biomarkers cutoffs: the importance of coincident neuropathological diseases. Acta neuropathologica. 2012;124:23-35.
[60] Frisardi V, Panza F, Seripa D, Farooqui T, Farooqui AA. Glycerophospholipids and glycerophospholipid-derived lipid mediators: a complex meshwork in Alzheimer's disease pathology. Progress in lipid research. 2011;50:313-30.
[61] Perttu EK, Kohli AG, Szoka FC, Jr. Inverse-phosphocholine lipids: a remix of a common phospholipid. Journal of the American Chemical Society. 2012;134:4485-8.
[62] Braverman NE, Moser AB. Functions of plasmalogen lipids in health and disease. Biochimica et biophysica acta. 2012;1822:1442-52.
[63] Fonteh AN, Ormseth C, Chiang J, Cipolla M, Arakaki X, Harrington MG. Sphingolipid metabolism correlates with cerebrospinal fluid Beta amyloid levels in Alzheimer's disease. PloS one. 2015;10:e0125597.
[64] Gross RW. High plasmalogen and arachidonic acid content of canine myocardial sarcolemma: a fast atom bombardment mass spectroscopic and gas chromatography-mass spectroscopic characterization. Biochemistry. 1984;23:158-65.
[65] Heppner FL, Ransohoff RM, Becher B. Immune attack: the role of inflammation in Alzheimer disease. Nature reviews Neuroscience. 2015;16:358-72.
[66] Rushworth JV, Hooper NM. Lipid Rafts: Linking Alzheimer's Amyloid-beta Production, Aggregation, and Toxicity at Neuronal Membranes. Int J Alzheimers Dis. 2010;2011:603052.
[67] Whiley L, Sen A, Heaton J, Proitsi P, Garcia-Gomez D, Leung R, et al. Evidence of altered phosphatidylcholine metabolism in Alzheimer's disease. Neurobiol Aging. 2014;35:271-8.
[68] McCoin CS, Knotts TA, Adams SH. Acylcarnitines--old actors auditioning for new roles in metabolic physiology. Nature reviews Endocrinology. 2015;11:617-25.
[69] Walter J, van Echten-Deckert G. Cross-talk of membrane lipids and Alzheimer-related proteins. Molecular neurodegeneration. 2013;8:34.
[70] Jones LL, McDonald DA, Borum PR. Acylcarnitines: role in brain. Progress in lipid research. 2010;49:61-75.
[71] Yin F, Yao J, Sancheti H, Feng T, Melcangi RC, Morgan TE, et al. The perimenopausal aging transition in the female rat brain: decline in bioenergetic systems and synaptic plasticity. Neurobiol Aging. 2015;36:2282-95.
[72] Stanley M, Macauley SL, Holtzman DM. Changes in insulin and insulin signaling in Alzheimer's disease: cause or consequence? The Journal of experimental medicine. 2016;213:1375-85.
[73] Kling MA, Trojanowski JQ, Wolk DA, Lee VM, Arnold SE. Vascular disease and dementias: Paradigm shifts to drive research in new directions. Alzheimer's & dementia : the journal of the Alzheimer's Association. 2013;9:76-92.
[74] Floegel A, Stefan N, Yu Z, Muhlenbruch K, Drogan D, Joost HG, et al. Identification of serum metabolites associated with risk of type 2 diabetes using a targeted metabolomic approach. Diabetes. 2013;62:639-48.
[75] Wang TJ, Larson MG, Vasan RS, Cheng S, Rhee EP, McCabe E, et al. Metabolite profiles and the risk of developing diabetes. Nature medicine. 2011;17:448-53.

[76] Wang TJ, Ngo D, Psychogios N, Dejam A, Larson MG, Vasan RS, et al. 2-Aminoadipic acid is a biomarker for diabetes risk. The Journal of clinical investigation. 2013;123:4309-17.
[77] Kawaguchi T, Nagao Y, Matsuoka H, Ide T, Sata M. Branched-chain amino acid-enriched supplementation improves insulin resistance in patients with chronic liver disease. International journal of molecular medicine. 2008;22:105-12.
[78] Ruiz HH, Chi T, Lindtner C, Hsieh W, Shin AC, Ehrlich M, et al. Increased susceptibility to metabolic dysregulation in a mouse model of Alzheimer's disease is associated with impaired hypothalamic insulin signaling and elevated BCAA levels. Alzheimer's & dementia : the journal of the Alzheimer's Association. 2016.
[79] Jha SK, Jha NK, Kumar D, Ambasta RK, Kumar P. Linking mitochondrial dysfunction, metabolic syndrome and stress signaling in Neurodegeneration. Biochimica et biophysica acta. 2016.
[80] Koliaki C, Roden M. Alterations of Mitochondrial Function and Insulin Sensitivity in Human Obesity and Diabetes Mellitus. Annual review of nutrition. 2016;36:337-67.

FIGURE LEGENDS

Figure 1. Clustering of pairwise metabolite correlations and association results with clinical variables.

A. Heatmap of Spearman correlations between the residuals of metabolite concentrations on the single metabolites. Metabolites are clustered using hierarchical clustering using the Euclidean distance metric. The clustering assigns metabolites to their biochemical class: amino acids, biogenic amines, short chain and long chain acylcarnitines, lyso-lipids, PC and SM. Significant clusters of acyl carnitines are outlined in blue and amines outlined in brown. **B.** Association results of the regression analyses. The distribution of association results of metabolites with clinical variables mirrors the correlation structure of the metabolites. *Abbreviations:* Path. $A\beta_{1-42}$ – Pathological A β_{1-42}; SDMA - Symmetric dimethylarginine; T4-OH-Pro – trans-4-Hydroxyproline; α-AAA – α-Aminoadipic acid; C0 – free carnitine; C*x:y* – acylcarnitines; C*x:y*-OH – hydroxylacylcarnitines, C*x:y*-DC – dicarboxylacylcarnitines; SM*x:y* – sphingomyelins; SM (OH) *x:y* – N-hydroxylacyloylsphingosyl-phosphocholine; PC – glycero-phosphatidylcholines (*aa*=diacyl, *ae*=acyl-alkyl); lysoPC – lyso-glycero-phosphatidylcholines (*a*=acyl); CN – cognitively normal; MCI –mild cognitive impairment; AD –Alzheimer disease;

Figure 2. Relationship between serum metabolites, clinical diagnosis, and $A\beta_{1-42}$ status

Serum PC ae 44:4 **(A)**, PC ae 44:4 **(B)** and C18 **(C)** concentrations stratified by clinical diagnosis and CSF $A\beta_{1-42}$–defined groups. The concentration of each metabolite is shown for each diagnosis Red: CN, Green: MCI, Blue: AD and by N. Abeta: normal concentrations of $A\beta_{1-42}$ (>192 pg/ml), and Path. Abeta: Pathological concentrations of $A\beta_{1-42}$ (<192 pg/ml), Y-axes are values for each metabolite. Scatterplot for ADAS-Cog13 and serum valine values (D). Black line and shading is the regression line and 95% confidence interval. **D and E** correlations between valine levels and cognitive decline in ADNI-1 and Rotterdam respectively.

Abbreviations: SDMA - Symmetric dimethylarginine; T4-OH-Pro – trans-4-Hydroxyproline; α-AAA – α-Aminoadipic acid; C0 – free carnitine; C*x:y* – acylcarnitines; C*x:y*-OH – hydroxylacylcarnitines, C*x:y*-DC – dicarboxylacylcarnitines; SM*x:y* – sphingomyelins; SM (OH) *x:y* – N-hydroxylacyloylsphingosyl-phosphocholine; PC – glycero-phosphatidylcholines (*aa*=diacyl, *ae*=acyl-alkyl); lysoPC – lyso- glycero-phosphatidylcholines (*a*=acyl).

Figure 3. Longitudinal associations for SM C20:2

(A) Cox hazards model of the association of conversion from MCI to AD. Black line: 1st tertile, Red line: 2nd tertile, Green line: 3rd tertile. Analysis was conducted using quantitative values and stratification by tertiles was used only for graphical representation.

(B) Association between baseline concentrations of SM 20:2 and longitudinal cognitive (ADAS-Cog13) and imaging (MRI: brain ventricular volume) changes during follow-up. Lines represent trajectories on subjects on the 25th percentile (black line), 50th percentile (red line), 75th percentile (green line) of baseline SM 20:2. Y-axes are ADAS-Cog13 score (left) and Ventricular Volume (right). Trajectories for these values are calculated based on the studied mixed-effects models.

Figure 4. Network model showing metabolic pathways correlated with the temporal evolution of biomarkers and clinical variables in AD.

A: Partial correlation network. Gaussian graphical model of metabolite concentrations showing reconstructed metabolic pathways and highlighting of the different modules involved in the steps along the temporal evolution of biomarkers and clinical variables in AD. Nodes in the network represent the metabolites, edges (lines) illustrate the strength and direction of their partial correlations. Only partial correlations significant after Bonferroni correction for all possible edges are included. Labels show the major classes of metabolites included in our study. Grey circles outline the modules highlighted in panel B.

B: Schematic diagram of the model of temporal evolution of biomarkers in AD according to Clifford and Holtzman [30], augmented with colored versions of the network from panel A. In these networks, nodes are highlighted according to the strength and direction of the metabolite's association with the respective clinical trait with blue as positive and red as negative (networks in temporal order from left to right: Pathological $A\beta_{1-42}$, T-tau, SPARE-AD, and ADAS-Cog 13). Significant associations are colored in dark blue/bright red, weaker (but at least nominally significant at 0.05) associations are displayed in fainter colors. Modules of metabolites implicated in the respective trait are highlighted by circles colored by their first occurrence in the temporal order following the color scheme of the time sequence on the bottom.
The partial correlation network for $A\beta_{1-42}$ (**Figure 4A**) highlighted direct correlations with short- and medium-chain SM and PC with ether-bonds suggesting a role for membrane structure and function, contact sites, and membrane signaling in amyloid pathology. There was a different pattern for tau (**Figure 4B**) with highlighted metabolites with long chain acylcarnitines and SM implicated in lipid metabolism showing association with T-tau level. The SPARE-AD and ADAS-Cog13 partial correlation networks were very similar suggesting associations of brain atrophy and cognitive decline with metabolic changes in BCAAs and short chain acylcarnitines that have been implicated in mitochondrial energetics as well as additional changes in lipid metabolism.

Figure 5. Co-expression subnetwork with direct and indirect interconnections between select metabolites

A co-expression sub-network focused on three metabolites also identified in the Rotterdam dataset (PC ae C40:3, Valine, and SM C20:2) was generated from the primary network (**Supplementary Figure 2**). The subnetwork shows these three metabolites have high correlations (red edges -lines-) and lower correlations (green edges lines-) to multiple modules via direct and indirect interconnections. Each module is denoted by a color representing a robust set of co-regulated metabolites in interconnected biochemical pathways e.g. orange module contained a subset of amines, green module consists of long chain acylcarnitines, teal, brown and blue modules contained exclusively PC and lyso PC, red module

contained SM and PC, grey module contained short chain acylcarnitines and other amines. Each node represents a metabolite. The edge (line) opacity is proportional to the Pearson correlation, i.e. i.e. lighter means weaker correlation value and darker means stronger correlation. The inter-module edges represent correlations and potentially indirect interactions among metabolites and biochemical pathways. The co-expression network captures all significant associations between metabolites and reveals a global correlation structure and interconnections among different modules that adds to our understanding of the disease network.

Table 1. Metabolites associated with clinical diagnosis, MRI or CSF biomarkers after Bonferroni correction.

Metabolites	MCI	AD	$A\beta_{1-42}$	T-Tau/$A\beta_{1-42}$	ADAS-Cog13	SPARE-AD
C12	0.9 (1.0)	-1.62 (1.0)	1.22 (1.0)	0.26 (0.33)	5.88 (0.073)	**0.87 (0.041)**
C14:1	10.79 (1.0)	-12.25 (1.0)	12.93 (1.0)	2.46 (0.05)	**52.21 (0.037)**	6.8 (0.1)
C16:1	1.25 (1.0)	-2.098 (1.0)	1.62 (1.0)	0.38 (0.091)	**9.4 (0.0037)**	**1.2 (0.020)**
C18	14.62 (1.0)	-19.27 (1.0)	21.62 (1.0)	**4.64 (0.0055)**	64.31 (0.5)	10.0095 (0.2)
PC ae C36:2	0.085 (0.33)	-0.082 (1.0)	**0.16 (0.007)**	**0.018 (0.013)**	0.23 (1.0)	0.027 (1.0)
PC ae C40:3	0.98 (1.0)	-3.27 (1.0)	**5.76 (0.017)**	0.49 (0.55)	2.72 (1.0)	0.26 (1.0)
PC ae C42:4	1.62 (0.063)	-1.51 (0.88)	**2.32 (0.017)**	0.19 (0.75)	3.63 (1.0)	**0.79 (0.049)**
PC ae C44:4	3.029 (1.0)	-3.37 (1.0)	**6.11 (0.016)**	0.6 (0.089)	11.24 (0.64)	**2.059 (0.037)**
SM (OH) C14:1	0.06 (1.0)	-0.054 (1.0)	**0.24 (0.044)**	0.027 (0.081)	0.2 (1.0)	0.016 (1.0)
SM C16:0	0.0065 (1.0)	-0.0074 (1.0)	**0.015 (0.016)**	**0.0017 (0.013)**	0.024 (1.0)	0.0037 (0.57)
SM C20:2	0.66 (1.0)	-1.082 (0.22)	0.74 (1.0)	**0.18 (0.047)**	**4.57 (<0.0001)**	0.4 (0.48)
α-AAA	-0.46 (1.0)	0.67 (1.0)	-0.68 (1.0)	-0.13 (0.098)	**-3.7 (0.0025)**	**-0.61 (<0.0001)**
Valine	-0.0038 (1.0)	0.0073 (0.079)	-0.004 (1.0)	-0.0006 (1.0)	**-0.028 (<0.0001)**	**-0.0039 (<0.0001)**

AD: Alzheimer disease; MCI: mild cognitive impairment; SPARE-AD: Spatial Pattern of Abnormalities for Recognition of Early AD.

The cells include the logistic (MCI and AD) and linear ($A\beta_{1-42,}$ T-Tau/$A\beta_{1-42}$, ADAS-Cog13, SPARE-AD) regression coefficients and, in parenthesis, the Bonferroni corrected p-value.

All model included age, and gender as covariates. *APOE* ε4 presence included in $A\beta_{1-42}$ model and education was included in the MCI, AD and ADAS-Cog13 models. A complete list is found in **Supplementary Table 2**.

Table 2. **Association of metabolites with longitudinal cognitive and MRI changes in MCI**.

Analytes	ADAS-Cog13 Change	Ventricle Volume Change	Progression MCI to AD Dementia
C12	0.091 (0.26)	0.11 (0.73)	1.37 (0.4)
C14:1	**1.39 (0.034)**	**7.085 (0.006)**	2.11 (0.22)
C16:1	0.15 (0.13)	0.67 (0.092)	1.9 (0.19)
C18	-0.16 (0.87)	1.94 (0.64)	2.41 (0.18)
PC ae C36:2	0.0075 (0.094)	0.031 (0.096)	**1.056 (0.012)**
PC ae C40:3	**0.38 (0.02)**	**1.5 (0.020)**	**5.98 (0.027)**
PC ae C42:4	**0.15 (0.04)**	**0.72 (0.013)**	**1.96 (0.042)**
PC ae C44:4	**0.49 (0.0076)**	**2.33 (0.0012)**	**5.89 (0.027)**
SM (OH) C14:1	**0.015 (0.04)**	**0.075 (0.01)**	**1.08 (0.025)**
SM C16:0	**0.0009 (0.025)**	**0.0037 (0.023)**	**1.004 (0.029)**
SM C20:2	**0.11 (0.0078)**	**0.48 (0.0035)**	**1.9 (0.0023)**
α-AAA	**-0.093 (0.022)**	-0.29 (0.087)	0.68 (0.061)
Valine	**-0.0006 (0.035)**	**-0.0027 (0.026)**	1.0 (0.27)

α-AAA: α-aminoadipic acid ; AD: Alzheimer disease; MCI: mild cognitive impairment. Table depicts the association between selected metabolites and longitudinal ADAS-Cog13 (Column 2) and ventricular volume (Column 3) in mixed effects models that were age, gender and *APOE* adjusted. In addition, the ADAS-Cog13 model was adjusted for education. Boxes contain the coefficients and, in parenthesis, the p-values. The last column (Column 4) presents the associations of the metabolites with progression from MCI to AD in Cox hazards models that included age, gender, education, and *APOE* as covariates.

Values represent hazard ratio and, in parenthesis, the p-values. Significant associations are shaded for an easier visualization. All p values were not multiple comparison corrected.

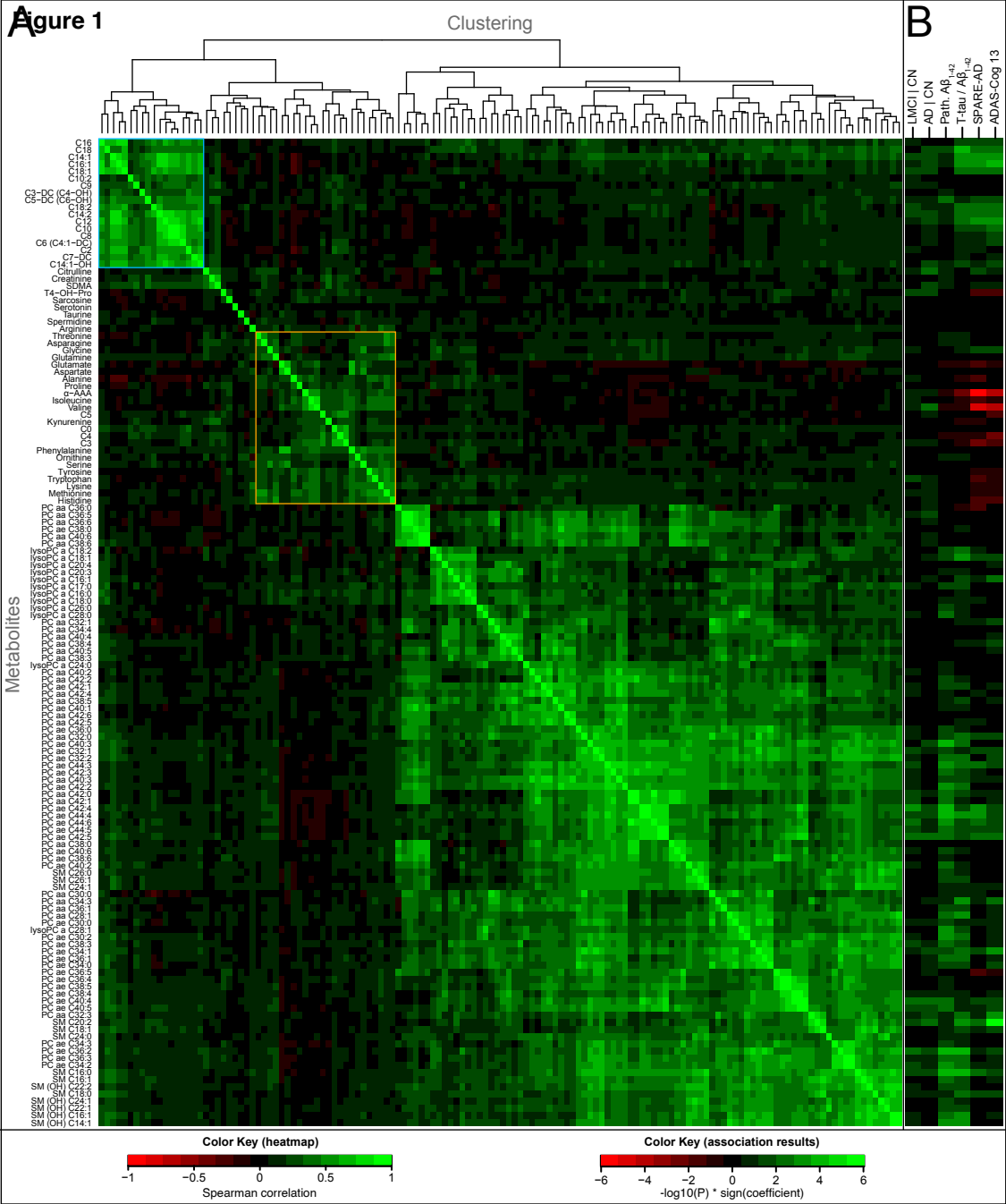
Figure 1
A
Clustering
B
LMCI | CN
AD | CN
Path. Aβ1-42
T-tau / Aβ1-42
SPARE-AD
ADAS-Cog 13
Metabolites
C16
C18
C14:1
C16:1
C18:1
C10:2
C9
C3-DC (C4-OH)
C5-DC (C6-OH)
C18:2
C14:2
C12
C10
C8
C6 (C4:1-DC)
C5
C7-DC
C14:1-OH
Citrulline
Creatinine
SDMA
T4-OH-Pro
Sarcosine
Serotonin
Taurine
Spermidine
Arginine
Threonine
Asparagine
Glycine
Glutamine
Glutamate
Aspartate
Alanine
Proline
α-AAA
Isoleucine
Valine
C5
Kynurenine
C0
C4
C3
Phenylalanine
Ornithine
Serine
Tyrosine
Tryptophan
Lysine
Methionine
Histidine
PC aa C38:0
PC aa C36:5
PC aa C38:6
PC ae C38:0
PC aa C40:6
PC aa C38:6
lysoPC a C18:1
lysoPC a C20:4
lysoPC a C20:3
lysoPC a C16:1
lysoPC a C17:0
lysoPC a C16:0
lysoPC a C18:0
lysoPC a C26:0
lysoPC a C28:0
PC aa C32:1
PC aa C34:4
PC aa C40:4
PC aa C38:4
PC aa C40:6
PC aa C38:3
lysoPC a C24:0
PC aa C40:2
PC aa C42:2
PC aa C42:1
PC aa C42:4
PC aa C38:5
PC ae C40:1
PC aa C42:6
PC aa C42:5
PC ae C36:0
PC aa C32:0
PC ae C40:3
PC ae C32:1
PC ae C32:2
PC ae C44:3
PC aa C42:3
PC ae C40:3
PC aa C42:1
PC aa C42:0
PC ae C42:1
PC ae C42:4
PC ae C44:4
PC ae C44:3
PC ae C44:5
PC ae C42:5
PC ae C38:0
PC ae C40:4
PC ae C38:6
PC ae C40:2
SM C26:1
SM C26:1
SM C24:1
PC aa C30:0
PC aa C34:3
PC aa C36:1
PC aa C28:1
PC aa C30:0
lysoPC a C28:1
PC aa C30:2
PC ae C38:5
PC ae C34:1
PC ae C36:1
PC ae C38:2
PC ae C36:0
PC ae C36:4
PC ae C38:5
PC ae C38:4
PC ae C40:4
PC ae C40:5
PC ae C32:2
SM C20:2
SM C18:1
SM C24:0
PC ae C34:3
PC ae C36:2
PC ae C36:3
PC ae C34:2
SM C16:2
SM C16:1
SM (OH) C22:2
SM C18:0
SM (OH) C24:1
SM (OH) C22:1
SM (OH) C16:1
SM (OH) C14:1
Color Key (heatmap)
−1
−0.5
0
0.5
1
Spearman correlation
Color Key (association results)
−6
−4
−2
0
2
4
6
-log10(P) * sign(coefficient)

Figure 2

Click here to download high resolution image

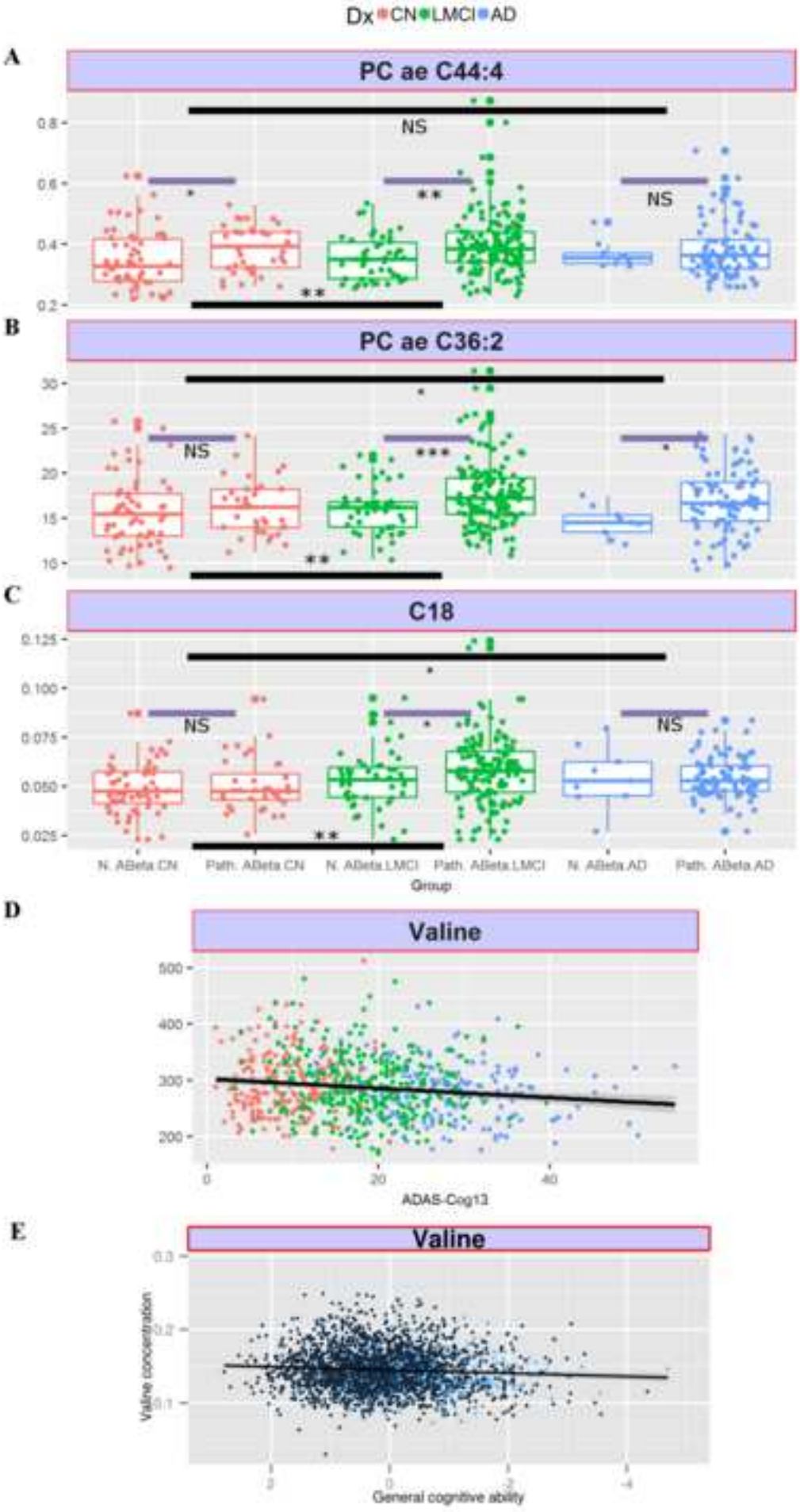

Figure 3

Click here to download high resolution image

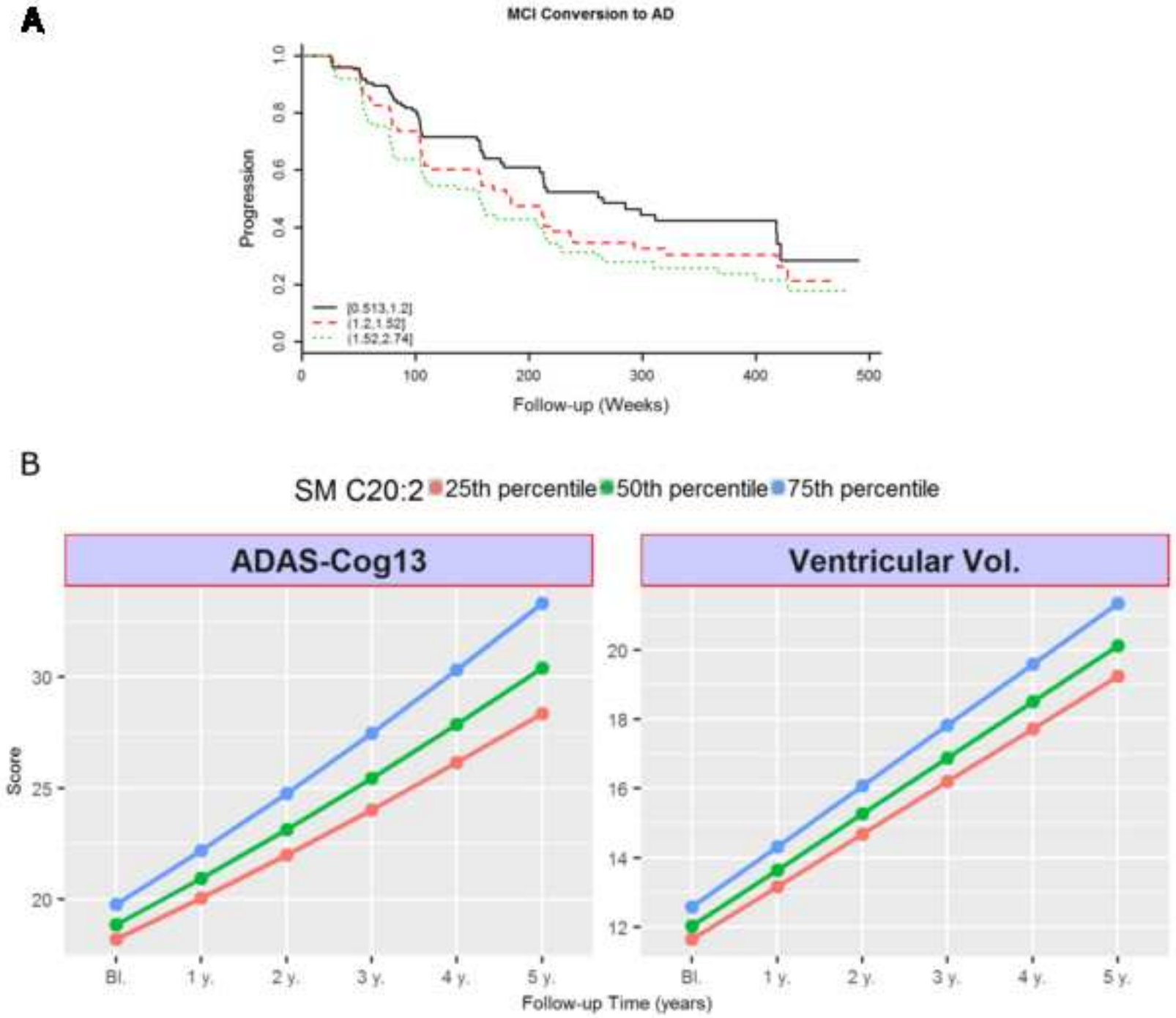

Figure 4

A

Negative Pcor
Positive Pcor

Long-chain sphingolipids

Short-chain sphingolipids

Glycerophospholipids

Amines & amino acids

Short-chain acylcarnitines

Long-chain acylcarnitines

PC ae C30:2
SM C16:0
SM C26:1
PC ae C40:3
PC aa C42:4
PC aa C40:2
SM (OH) C16:1
lysoPC a C28:1
SM C16:1
SM (OH) C22:2
SM C24:1
SM (OH) C14:1
SM (OH) C22:1
SM C26:0
lysoPC a C28:0
SM (OH) C24:1
SM C18:0
lysoPC a C24:0
PC aa C40:3
SM C18:1
lysoPC a C26:0
SM C24:0
PC ae C40:2
SM C20:2
PC aa C32:3
PC aa C28:1
PC aa C42:6
PC aa C42:5
PC ae C42:2
PC aa C34:3
PC ae C42:4
PC ae C42:3
PC ae C44:4
PC ae C44:3
PC ae C42:1
PC aa C34:4
PC aa C40:4
PC ae C30:0
PC ae C40:1
PC aa C40:5
PC ae C44:5
PC aa C36:5
PC aa C36:6
PC ae C42:5
PC aa C30:0
PC aa C38:5
PC aa C32:0
PC ae C44:6
PC ae C38:0
PC ae C40:5
PC ae C32:2
PC ae C32:1
PC aa C42:1
PC ae C40:4
PC aa C40:6
PC aa C42:2
PC ae C34:0
PC aa C42:0
PC ae C40:6
PC aa C32:1
PC ae C36:0
PC aa C38:6
PC aa C36:0
PC aa C38:0
lysoPC a C16:1
PC ae C34:1
PC ae C36:1
PC ae C38:4
PC ae C38:6
lysoPC a C17:0
lysoPC a C16:0
PC ae C36:5
PC aa C36:1
PC aa C38:4
PC ae C38:5
PC ae C34:3
PC ae C36:2
lysoPC a C18:0
lysoPC a C18:1
PC ae C36:4
lysoPC a C18:2
PC aa C38:3
PC ae C34:2
PC ae C36:3
lysoPC a C20:4
lysoPC a C20:3
PC ae C38:3

Methionine
Tyrosine
Threonine
Asparagine
Tryptophan
Kynurenine
SDMA
Citrulline
Creatinine
Glycine
Ornithine
Arginine
Serine
Lysine
Aspartate
Glutamate
Phenylalanine
Glutamine
Histidine
Sarcosine
Proline
Taurine
α-AAA
Isoleucine
Alanine
Spermidine
Serotonin
T4-OH-Pro
Valine

C5
C4
C3
C0
C3-DC (C4-OH)
C2
C7-DC
C14:1-OH
C16
C18:1
C18
C5-DC (C6-OH)
C6 (C4:1-DC)
C16:1
C12
C18:2
C14:1
C10
C8
C14:2
C9
C10:2

B

Pathological $A\beta_{1-42}$
T-tau
SPARE-AD
ADAS-Cog 13

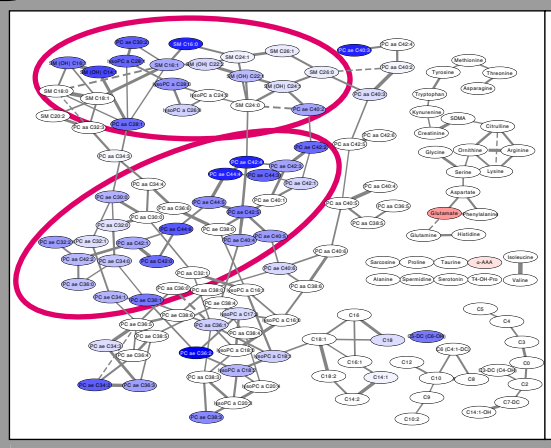
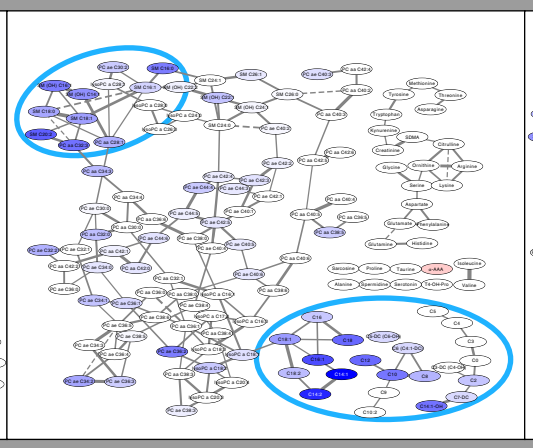
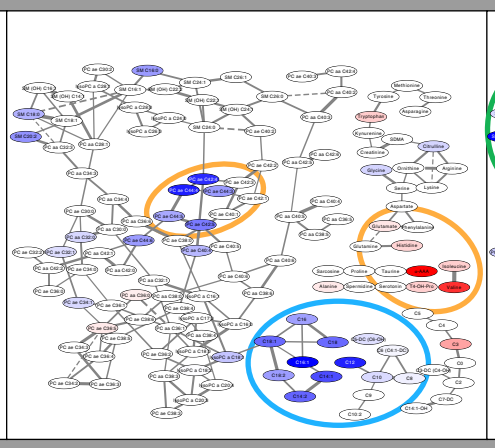
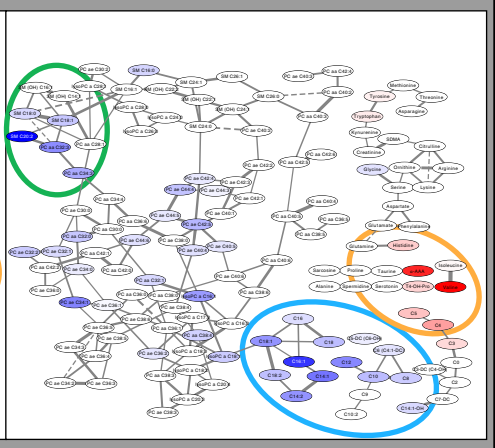

Biomarker

Pathological $A\beta_{1-42}$

T-tau

SPARE-AD

ADAS-Cog 13

Time

Figure 5

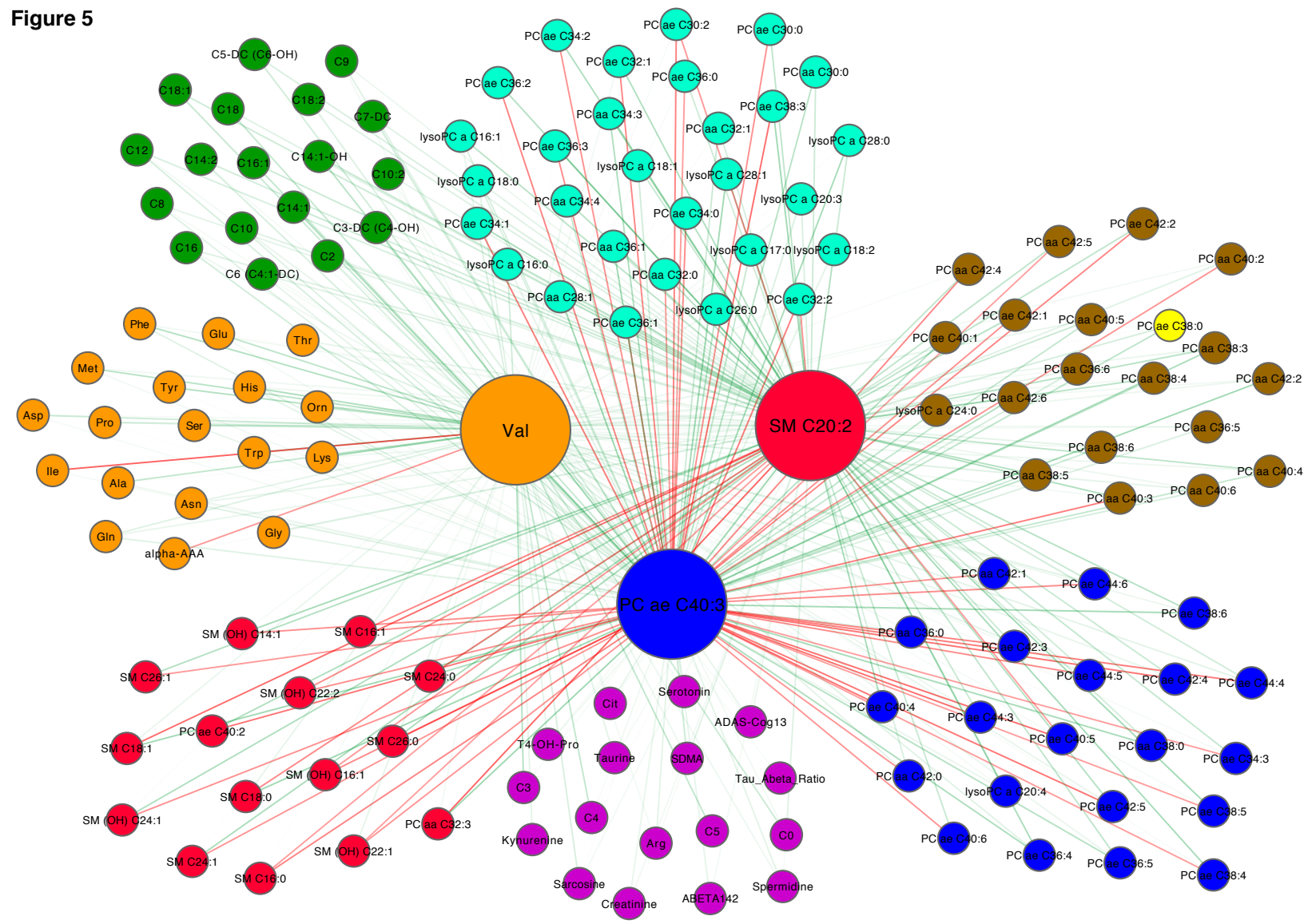
Val
SM C20:2
PC ae C40:3
C5-DC (C6-OH)
C9
C18:1
C18
C18:2
C7-DC
C12
C14:2
C16:1
C14:1-OH
C10:2
C8
C14:1
C10
C3-DC (C4-OH)
C16
C2
C6 (C4:1-DC)
PC ae C34:2
PC ae C30:2
PC ae C30:0
PC ae C32:1
PC ae C36:0
PC aa C30:0
PC ae C36:2
PC ae C38:3
PC aa C34:3
PC aa C32:1
lysoPC a C28:0
lysoPC a C16:1
PC ae C36:3
lysoPC a C18:1
lysoPC a C28:1
lysoPC a C18:0
PC aa C34:4
lysoPC a C20:3
PC ae C34:0
PC ae C34:1
PC aa C36:1
lysoPC a C17:0
lysoPC a C18:2
lysoPC a C16:0
PC aa C32:0
PC aa C28:1
lysoPC a C26:0
PC ae C32:2
PC ae C36:1
Phe
Glu
Thr
Met
Tyr
His
Orn
Asp
Pro
Ser
Trp
Lys
Ile
Ala
Asn
Gln
Gly
alpha-AAA
PC ae C42:2
PC aa C42:5
PC aa C40:2
PC aa C42:4
PC ae C42:1
PC aa C40:5
PC ae C38:0
PC aa C40:1
PC aa C38:3
PC aa C36:6
PC aa C38:4
PC aa C42:2
PC aa C42:6
lysoPC a C24:0
PC aa C36:5
PC aa C38:6
PC aa C38:5
PC aa C40:4
PC aa C40:3
PC aa C40:6
PC aa C42:1
PC ae C44:6
PC ae C38:6
PC aa C36:0
PC aa C42:3
PC ae C44:5
PC ae C42:4
PC ae C44:4
PC ae C40:4
PC ae C44:3
PC ae C40:5
PC aa C38:0
PC ae C34:3
PC aa C42:0
lysoPC a C20:4
PC ae C42:5
PC ae C38:5
PC ae C40:6
PC ae C36:4
PC ae C36:5
PC ae C38:4
SM (OH) C14:1
SM C16:1
SM C26:1
SM C24:0
SM (OH) C22:2
PC ae C40:2
SM C18:1
SM C26:0
SM (OH) C16:1
SM C18:0
SM (OH) C24:1
PC aa C32:3
SM C24:1
SM (OH) C22:1
SM C16:0
Cit
Serotonin
ADAS-Cog13
T4-OH-Pro
Taurine
SDMA
Tau_Abeta_Ratio
C3
C4
Kynurenine
Arg
C5
C0
Sarcosine
Creatinine
ABETA142
Spermidine

Supplementary files

Click here to download Supplementary files: Jon Suppl 1 Jan 25 UPLOAD highlighted FINAL FINAL.docx

Supplementary files

Click here to download Supplementary files: Supplementary_Material_File_2_Heatmap Jan 25 UPLOAD.xlsx

Supplementary files

Click here to download Supplementary files: For UPLOAD Jan 25 Supplemental Fig 2.pdf

Supplementary files

Click here to download Supplementary files: Supplementary_Material_File_3_ Data_for_network Jan 25 UPLOAD.xlsx